EUROPEAN ORGANIZATION FOR NUCLEAR RESEARCH

LIGHT MESONS WITH OPEN AND HIDDEN STRANGENESS

M.A. Faessler
Sektion Physik, Ludwig-Maximilians-Universität, D-80799 Munich, Germany

Abstract

Mesons are the most fundamental objects allowing a study of quark and gluon confinement and, more generally, the strong interaction at low energy. The spectroscopy of light mesons is a challenge: the glueballs predicted on the basis of Quantum Chromodynamics are expected amidst the light mesons. However, identifying light mesons and determining their quantum numbers are particularly difficult tasks due to their extremely short lifetimes. The strangeness quantum number is easy to detect and indicates the presence of a strange quark. Thus the field of (openly) strange mesons is relatively well explored. However that of mesons with hidden strangeness, more directly relevant to the glueball search, still needs more experimental input, in particular from studies of final states with kaon–antikaon pairs.

Three lectures at the Nato Advanced Study Institute
Hadron Spectroscopy and the Confinement Problem
Swansea, Wales, June 27–July 8, 1995

1 INTRODUCTION

Niels Bohr first heard of the Balmer formula, known since 1885 on 7 February 1913. By March 6, he had completed a paper containing its interpretation. This event marked the beginning of quantum mechanics [1]. The spectral lines of hydrogen, the simplest atom, bound by the electromagnetic force, played a leading role at several stages in the development of the present theory of the electromagnetic force, Quantum ElectroDynamics (QED).

Now, if you learn during this summer school, perhaps for the first time, about the spectra of mesons — the simplest systems bound by the strong force — it is not very likely (although a great hope of the teachers) that in a month from now you will come up with an elegant theory explaining all their properties.

Firstly, all experts are convinced that we already have the best theory of strong interactions, Quantum ChromoDynamics (QCD). The ground states of mesons and baryons have played a key role in the first big step on the way to QCD, the conception of the quark model. But the proper domain of QCD nowadays concerns rare processes, where quarks are asymptotically free. 'Asymptotically' implies that truly free quarks have never been observed; they are confined to hadrons. And our best theorists have so far failed to apply their pet theory (QCD) to the simplest bound states. In this latter domain of 'non-perturbative' QCD, the calculations become so complex that nobody has yet succeeded in deriving a truly quantitative description of meson spectra from QCD. Clearly, one may comfortably live with such a situation and look for other interesting objects like the Higgs particles. However, there have been quite a few similar situations in history which serve as a warning. Think of Ptolemaios who had a simple and elegant theory postulating just epicycles and epicentres as basic elements of the orbits of stars and planets. As more and more orbits were observed, application of the theory became increasingly complex. In the end the theory turned out to be a rather bad approximation of nature.

The second reason for being unable to find an elegant description of the spectra of mesons may be that the experimental input is too fragmented. Ultimately, the strength of the interaction is to blame for this, as it is for the difficulty in applying QCD to non-perturbative processes. As the interaction is so strong, the meson states, whenever their decay is induced by the strong force, are extremely short-lived. Bound by the strongest of all interactions, their constituents stay together for a shorter time than any other bound state of nature. Their extremely short lifetime renders identification particularly difficult. Detected through their decay, these bound states do not show up as narrow, distinct lines on the scale of invariant energy or mass of the decay products, but as broad diffuse enhancements of intensities, called resonances. (The line width Γ is inversely proportional to the lifetime, $\Gamma = \hbar/\tau$). In general, the various resonances with different quantum numbers produced in a given process overlap in energy. This renders the determination of the quantum numbers cumbersome. Thus, even after several decades of research the measurements are still not as complete as one would wish.

The subjects of these three lectures are light strange mesons, i.e. those containing a strange quark (s) or antiquark ($\bar{s}$), and mesons with hidden strangeness, i.e. those containing an ($\bar{s}s$)-pair. The following two chapters are fairly fundamental. They are intended as an introduction for an audience of students or physicists with a general physics education but not yet experts in particle physics and hadron spectroscopy. Chapter 2 ends with a survey of known quantum states of light mesons, which can be considered as a starting point for experts in the field. Chapter 3 outlines the experimental methods of meson spectroscopy, in particular detection of mesons with strange quarks. Chapter 4 is

a review of some of the open problems in the special field of strange and hidden strange light-mesons. The lectures, as they are given by an experimentalist, focus on experimental rather than theoretical work in the field of meson spectroscopy.

2 QUANTUM STATES OF LIGHT MESONS

2.1 The basic constituents

The systematics of hadrons (mesons and baryons) first observed in the 1950s and 1960s, have led to the **quark model**, which describes hadrons as composite objects made of hypothetical constituents, the quarks. These quarks had to carry the quantum numbers or fractions thereof which had been observed to be conserved in strong interactions, such as charge, spin, baryon number (also conserved in other interactions), isospin and strangeness. Since these are lectures on strange mesons it seems appropriate to recall briefly the discovery of **strangeness**. Soon after the existence of hyperons (unstable particles heavier than a nucleon) and K mesons (particles with masses between those of pions and nucleons) had been established through various decay modes, and the rate of production had been studied in a pion beam at the Brookhaven Cosmotron, it was noted that there was a problem. These particles were copiously produced by the strong interaction, at a rate of 10% of that for pions; but their decay was very slow (mediated by the weak interaction). As an explanation, Pais (1952) and Nambu introduced the rule of 'associated production', requiring hyperons and kaons to be produced in pairs by strong interaction, for example

$$\pi^+ + n \rightarrow \Lambda + K^+ \quad .$$

Inverting this process, the strong decay of Λ and K would be

$$\Lambda \rightarrow \pi^+ + n + K^- \quad \text{and} \quad K \rightarrow \pi^+ + n + \bar{\Lambda}$$

Both decays are forbidden by energy conservation. An explanation of the rule was given by Gell-Mann (1953) and Nishijima (1955) by inventing a new additive quantum number called strangeness (S), conserved in strong interactions. The Λ and K^- were assigned the same S, and K^+ was given the opposite S. Strangeness non-conservation in the decays rules out the action of the strong force; since the decays are left to the weak force, they are slow.

The **point-like nature** and other properties of the quark constituents were inferred from many subsequent experiments which studied hard interactions involving hadrons. 'Hard' means that high-momentum transfers are involved; to probe short distances, large momentum transfers are needed according to the Heisenberg uncertainty relations. The present theory of strong interactions (QCD) has emerged as the best description of all these experimental data. Ironically, the 'stable' hadrons and their lowest excitations, which started this chain of progressive understanding, are the objects where the theory fails most strikingly to produce a quantitative description. Nonetheless, the qualitative description provided by QCD for the laws governing how hadrons are built from basic constituents is a good starting point, which we will use as a guideline. Of course, in doing so we are starting from the back end of research, i.e. from the theory instead of the empirical basis which led to the theory. However, there is a definite advantage to this approach to the subject: the quantum numbers and names of mesons are much more easily memorized if one already has an idea of how the mesons are formed.

QCD is a gauge theory modelled on QED and incorporating the quark model. It describes a world where the elementary fermions are the quarks and antiquarks, with spin quantum number 1/2, baryon number +1/3 for quarks and −1/3 for antiquarks,

charge $\pm 1/3$ or $\pm 2/3$ of the proton charge and a quantum number, called flavour, which is peculiar to each quark species (Table 1).

Table 1: Quarks, their quantum numbers and masses. Flavour quantum numbers: I_z = isospin z-component, S = strangeness, C = charm, B = bottomness, T = topness, Q = charge in units of the proton charge, m = current quark mass, M = constituent quark mass. The corresponding antiquarks have equal masses but opposite signs for all other quantum numbers.

Name	Symbol	I_z	S	C	B	T	Q	m[MeV/c^2]	M [MeV/c^2]
down	d	$-1/2$	0	0	0	0	$-1/3$	10 ± 5	300 ± 100
up	u	$+1/2$	0	0	0	0	$+2/3$	5 ± 3	300 ± 100
strange	s	0	-1	0	0	0	$-1/3$	200 ± 100	450 ± 100
charm	c	0	0	1	0	0	$+2/3$	1300 ± 300	≈ 1500
bottom	b	0	0	0	-1	0	$-1/3$	4300 ± 200	≈ 5000
top	t	0	0	0	0	1	$+2/3$	174000 ± 1700	

An additional property of the quarks, called colour charge, plays an analogous role for the strong interaction, as does electric charge for the electromagnetic interaction and mass for gravitation. Colour charge can have 3 different non-zero values. The sum of 3 different colours, or of a colour and the corresponding anticolour, yields zero, which is analogous to the additive mixing of three primary colours, hence the name 'colour charge'. The quanta of the strong force field, analogous to the photon (the quantum of the electromagnetic field), are the **gluons**. There are $3 \times 3 - 1 = 8$ gluons because there are three colours and three anticolours. Gluons have a spin quantum number of 1; their electric charge, baryon number and flavour quantum numbers are all zero. But they carry colour charges, and as a consequence gluons interact directly not only with quarks and antiquarks but also with other gluons. For comparison, the gauge boson of QED, the photon, can interact with another photon only via charged particles.

Neither quarks nor gluons have ever been observed as free particles. Therefore, they are believed to be confined within hadrons. **Confinement** is built into the theory by assuming that free particles have to be colourless or, more precisely, singlets with respect to colour SU(3) transformations.

2.2 Hadrons

A hadron is, according to QCD, a very complex object, consisting of an indefinite number of quarks and/or gluons such that together they form a colour singlet. Two distinctions must be made when talking about the constituents of hadrons: between **valence** quarks and **sea** quarks, and between **current** quarks and **constituent** quarks. Valence quarks are those responsible for the quantum numbers like charge, baryon number, isospin and strangeness. Sea quarks are present as pairs of a quark and the corresponding antiquark, so that they do not contribute to these quantum numbers. They may be considered as vacuum fluctuations. The strong field, whose quanta are the gluons, creates virtual quark–antiquark pairs as the electromagnetic field creates electron–positron pairs (the latter effect is known from the Lamb shift in the hydrogen atom). The number of sea quarks is indefinite. Current quark is synonymous with elementary quark. The usual description of a constituent quark is that it contains an elementary valence quark

surrounded by a 'polarization cloud' of sea-quark pairs and gluons. A similar distinction is made between elementary gluon and **constituent gluon**.

The known hadrons are divided into three classes: mesons, baryons and antibaryons, according to their baryon number, which has been observed to take the values 0, +1 and –1, respectively. The baryon number equals the sum of the baryon numbers of the valence quarks contained in the hadron. The simplest hadrons are the **mesons**, which contain a valence quark q_i and a valence antiquark $\bar{q}_j$, and an indefinite number of sea-quark pairs and gluons. The indices i and j stand for the five quark flavours — the sixth, recently-discovered top quark is too short-lived (although elementary!) to build a hadron. Using the notion of constituent quarks, these mesons, called **normal** or **quark-model mesons** consist of a constituent quark and a constituent antiquark.

Baryons like protons or neutrons contain 3 valence quarks, and antibaryons contain 3 valence antiquarks. The proton consists of uud, the neutron of udd and the antiproton of $\bar{u}\bar{u}\bar{d}$. According to the prescription mentioned above, the colour combination has to be singlet. This would not be possible for one or two single quarks, but it is for the combination to a normal meson, baryon or antibaryon. In addition to these three classes, there ought to be other possible combinations to obtain a colour singlet; for instance, two or three constituent gluons ('gluonium' or 'glueball'), quark, antiquark and a constituent gluon ('hybrid'), or two quarks and two antiquarks (4-quark meson). These other combinations, predicted in principle by QCD, are assigned to the category **'exotic' mesons**, since they have not yet been proven to exist.

2.3 Constructing mesons: spatial quantum numbers

The normal mesons are the simplest systems bound by strong interaction. Given the fact that single free quarks or gluons have not been observed, we should expect that these objects are particularly important for an understanding of both the strong force and the nature of the constituents. We should expect them to play a similar role in the development of the theory of strong interactions as did the **hydrogen atom** in the development of QED. However, so far this has not been the case. The mesons, in particular the light mesons built from the light quarks (u, d, and s) and their antiquarks, have scarcely penetrated the textbooks of particle physics. The reasons have already been indicated above: the lack of a true understanding and the incompleteness of the data.

Not only the key role of the H-atom in the development of QED, but also its level scheme (Fig. 1) can serve as a reference. It is useful for a comparison because it is the best-known scheme of quantum states. Moreover, the spin and orbital angular momentum structure of mesons is very similar to that of the H atom. Both bound systems consist of two fermions (spin 1/2). For an orbital angular momentum L = 0 between the two fermions there are two states, the 'para' configuration with antiparallel spins, total spin S = 0 and total angular momentum J = 0, and the 'ortho' configuration with S = J = 1. For a relative orbital angular momentum L = 1, there are 4 states with total angular momenta J = 0, 1, 1, and 2. Using a notation which is customary for atoms with several electrons $^{2S+1}L_J$ where L = 0, 1, 2,.., is expressed by the letters S, P, D,.., the corresponding six meson states are:

$$^1S_0,\ ^3S_1,\ ^3P_0,\ ^3P_1,\ ^1P_1,\ ^3P_2.$$

A different notation, also frequently applied for mesons, uses the total angular momentum J, the parity P and the C-parity C, when the state is an eigenstate of the charge conjugation operator **C**. The strong interaction is symmetric for an inversion of the

coordinates, i.e. reflection at the origin or the parity operation **P**. The eigenvalue P can be ± 1. For a normal $(q_i \bar{q}_j)$ meson it is given by the expression

$$P = (-1)^{L+1} \ .$$

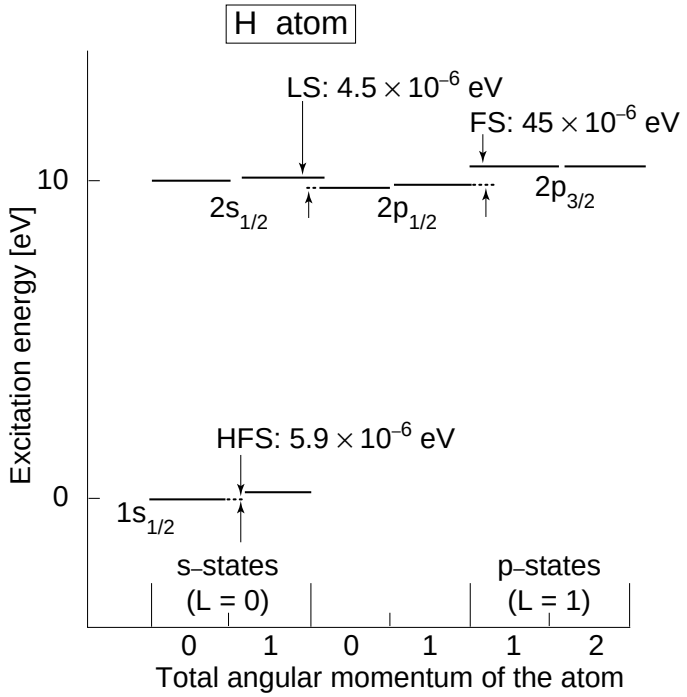

Figure 1: The 8 lowest energy levels of the hydrogen atom. Horizontal axis: total angular momentum (sum of electron and proton spin and orbital angular momentum). Vertical axis: excitation energy relative to the n = 1 ground states. HFS = hyperfine splitting, LS = Lamb shift, FS = fine structure splitting

The factor $(-1)^L$ is due to the action of **P** on the spatial wave function and the additional factor –1 is due to the opposite intrinsic parities of fermions and antifermions (derived from the Dirac equation). The charge conjugation **C** transforms a particle into its antiparticle, $\mathbf{C}u = \bar{u}$, $\mathbf{C}d = \bar{d}$, $\mathbf{C}s = \bar{s}$. The C-parity is another conserved quantum number. Mesons which consist of a quark q_i and the corresponding antiquark $\bar{q}_i$ are eigenstates of **C** and of the total spin S. The C-parity is given by

$$C = (-1)^{L+S} \ .$$

This relation is derived by writing the wave function as a product of a spin part, a spatial part and a flavour part and applying the generalized Pauli principle, which requires the complete wave function to be antisymmetric with respect to the interchange of the two fermions.

With these relations we can now make the transformation from one notation to the other (Table 2).

The two axial-vector mesons are distinguished by their C-parity in the case of eigenstates of **C**: $J^{PC} = 1^{++}$ for $^3P_1$ and $J^{PC} = 1^{+-}$ for $^1P_1$. For mesons which are not eigenstates of **C**, like the K mesons, the two components $^3P_1$ and $^1P_1$ can mix. These mesons are eigenstates of L and J but not of S.

Table 2: Names and quantum numbers of normal mesons for L = 0 and L = 1

Name	J^P	$^{2S+1}L_J$
pseudoscalar	0^-	$^1S_0$
vector	1^-	$^3S_1$
scalar	0^+	$^3P_0$
axial	1^+	$^3P_1$ or $^1P_1$
tensor	2^+	$^3P_2$

Only the eight lowest-energy spatial configurations of mesons are discussed above; they correspond to those shown for the hydrogen atom in Fig. 1, which included the first radial excitations of the S states and the lowest orbital excitations with L = 1. Of course, as for the H atom, higher orbital and radial excitations ($L \geq 2$ and $n \geq 2$) are possible.

All the listed quantum number combinations are typical for normal mesons. Several J^{PC} combinations are excluded even if higher orbital angular momenta are considered, e.g. $J^{PC} = 0^{--}$ or 1^{-+}. These **exotic** J^{PC} combinations are, however, possible for gluonia and hybrids since the gluon constituent has integer spin ($J^{PC} = 1^{--}$). If found, they would constitute direct proof of the existence of exotic mesons.

2.4 Constructing mesons: flavour quantum numbers and the nonet

Combining the first three quarks with the first three antiquarks yields a nonet of normal quark model mesons for each spatial configuration (Fig. 2a). They are called the **light mesons**, whereas those containing at least one charm or bottom quark are called heavy. There is, for instance, a nonet of vector mesons, as shown in Fig. 2b. All the (additive) flavour quantum numbers and the charge can be obtained by adding the corresponding quantum numbers of the quark constituents. The 6 states at the corners of the hexagon are easily distinguishable by their external quantum numbers, strangeness and charge. The three states in the centre of the hexagon, with $S = I_z = 0$ are less easy to identify. Their wave functions are superpositions of the 3 combinations $\bar{u}u, \bar{d}d, \bar{s}s$. They are shown, for the ideal case of perfect SU(2) and SU(3) symmetry, in Fig. 2a and for a real case, the vector mesons, in Fig. 2b.

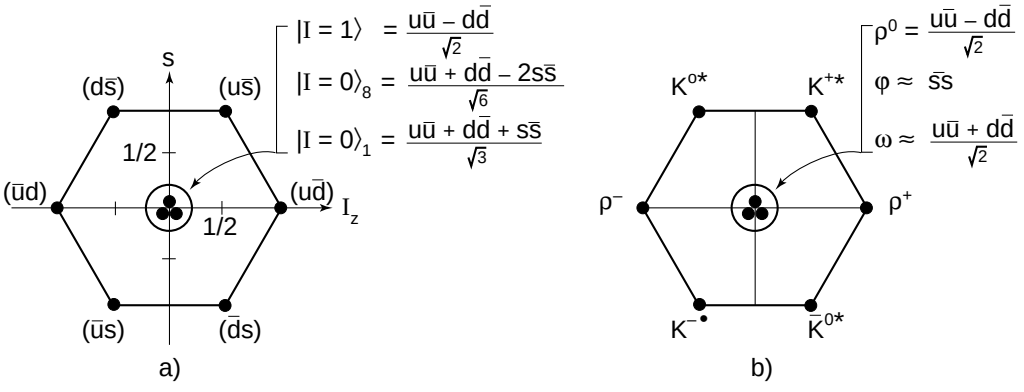

Figure 2: The flavour nonet of mesons and the wave functions of the three states in the centre (horizontal axis isospin z-component I_z; vertical axis strangeness S). For the case of (a) ideal SU(2) and SU(3) symmetry and (b) the vector mesons, where the two isosinglet states are 'ideally' mixed, i.e. almost pure $s\bar{s}$ and $\bar{u}u + \bar{d}d$.

Without describing details of SU(2) and SU(3) which can be found in textbooks, the following explanation is intended as a mnemonic for the signs and weights contained in these wave functions. It is assumed that the isospin formalism is known, e.g. from nuclear physics courses. It is an empirical fact that the strong interaction does not distinguish between up and down quarks, to a very good approximation. (QCD incorporates this fact by the assumption that the strong interaction only couples to the colour charge of quarks and by having nearly equal masses of up and down quarks.) We may then consider the up and down quarks as the two states of an isospin doublet $(u, d) = (+1/2, -1/2)$, as is done (following Heisenberg's suggestion) for p and n in nuclear physics, in analogy to the two orientations up and down for a spin 1/2 particle. The doublet of the antiquarks is $(+1/2, -1/2) = (\bar{d}, -\bar{u})$ with a minus sign in front of $\bar{u}$, such that this doublet transforms properly under isorotations [2]. Combining the doublet with the antidoublet, we obtain 4 states (as in atomic physics when combining two spin doublets, i.e. combining two particles with spin $s = 1/2$ and $s_z = \pm 1/2$). Remember the four states obtained when the spins of two electrons are added together. Using the notation $\uparrow, \downarrow$ for spin up and down, $s_z = +1/2$, $-1/2$), the four spin wave functions are

$$\begin{aligned} |S = 0, S_z = 0\rangle &= (\uparrow\downarrow - \downarrow\uparrow)/\sqrt{2} \\ |S = 1, S_z = +1\rangle &= \uparrow\uparrow \\ |S = 1, S_z = -1\rangle &= \downarrow\downarrow \\ |S = 1, S_z = 0\rangle &= (\uparrow\downarrow + \downarrow\uparrow)/\sqrt{2} \quad . \end{aligned}$$

For the combination of our two isospin doublets, or more precisely, of an isodoublet with the isodoublet of its antiparticles, the only difference is that the signs in the wave functions with $I_z = 0$ are reversed because of the minus sign in front of the $\bar{u}$ quark:

$$\begin{aligned} |I &= 0, I_z = 0\rangle = |\bar{d}d + \bar{u}u\rangle/\sqrt{2} \\ |I &= 1, I_z = 0\rangle = |\bar{d}d - \bar{u}u\rangle/\sqrt{2} \quad . \end{aligned}$$

The first state is the isosinglet, which behaves like a scalar under SU(2) transformations, i.e. rotations in isospace. The second state is the neutral partner of the three isovectors (the isotriplet); for the case of pseudoscalar ($J^P = 0^-$) mesons this triplet consists of the three pions, π^+, π^0, π^-.

Now let us add a third quark, the strange quark. Four additional particles are obtained at the corners, the K mesons with **'open' strangeness** and two more particles in the centre, ($S = I_z = 0$) with **'hidden' strangeness** (Fig. 2). These 6 meson species form the subject of the present lectures.

The nonet of mesons is divided into a singlet and an octet. The combination

$$|I = 0\rangle_1 = |\bar{u}u + \bar{d}d + \bar{s}s\rangle/\sqrt{3}$$

behaves like a scalar under flavour-SU(3) transformations; it is the SU(3) singlet, and the subscript '1' refers to this property. (For the colour SU(3) of QCD, it is the corresponding colour singlet which is realized in free hadrons; it is found by combining either three different quark colours or colour and anticolour. Correspondingly, there are only 8 coloured gluons, since one SU(3) combination is colourless.)

With SU(2) symmetry for u and d, the state $|I = 1, I_z = 0\rangle$ remains the same as for SU(2) and forms the second state in the centre of the nonet.

The third state in the centre can now be found by requiring orthogonality to the first two states $|I = 1, I_z = 0\rangle$ and $|I = 0\rangle_1$:

$$|I = 0\rangle_8 = |\bar{u}u + \bar{d}d - 2\bar{s}s\rangle/\sqrt{6} \quad .$$

The index 8 refers to the fact that it is a member of the octet. Thus it can be seen that hidden strangeness is mixed with $\bar{u}u + \bar{d}d$ in a certain ratio for this ideal SU(3) case. If nature were flavour-SU(3) symmetric, all the members of the octet would be mass degenerate. This is not the case, the presumed reason being the significantly heavier mass of the s quark compared to the masses of the u and d quarks (see Table 1). Nature also mixes the two states $|I = 0\rangle_1$ and $|I = 0\rangle_8$. We will return to the octet–singlet mixing angle later. For the moment, let us assume that flavour SU(3) is not a good symmetry, unlike SU(2) for up and down quarks. This explains why in Table 1 the up and down quarks appear to play a special role. Instead of assigning them the quantum numbers 'upness' and 'downness', they were labelled $I_z = +1/2, -1/2$. As a consequence of SU(2) symmetry, total isospin I and I_z are good quantum numbers, i.e. conserved in strong interactions, and hadrons with the same I but different I_z are approximately mass degenerate.

Thus the mesons of every nonet can be grouped into four multiplets of particles with (almost) degenerate masses:

- the 3 isovectors (an isotriplet, I = 1);
- the two doublets (I = 1/2) of K mesons, $K^+, K^0, \bar{K}^0, K^-$;
- the first isosinglet (I = 0);
- the second isosinglet (I = 0).

The mesons 'constructed' in the last two sections were all **normal or quark-model mesons**. So far, the existence of mesons with **flavour-exotic** quantum numbers, like strangeness S = 2 or charge = 2, has not been proven. It would indicate that bound states of more than one quark and antiquark exist. In addition to the notion flavour-exotic and the notion J^{PC}-exotic explained above, there is also the notion **crypto-exotic** for conceivable meson states which have the same quantum number combinations as normal mesons but a different composition, for instance, gluonia with $J^{PC} = 0^{++}, 2^{++}$ or 0^{-+}, and S = I = 0.

2.5 A survey of all mesons

We are now ready for a general survey of all mesons observed so far, in four decades of research, after which the lectures will specialize in the strange sector. A complete and up-to-date survey of mesons with reference to every single measurement can be found in the Review of Particle Properties (the 'bible' of the particle physicists) by the Particle Data Group (PDG) [3], pp. 1443–1672. There is also a handy resumé of the quark model in this review, pp. 1319ff. The book is indispensible for any meson or hadron expert. Figure 3 compares the level schemes of the majority of mesons as compiled in the meson summary table of the PDG [3]. This figure also serves to introduce all the symbols for the different mesons (According to E. Fermi, you have to be a botanist to remember these names). Only states with $L \leq 1$ and $n \leq 2$ are displayed in Fig. 3, as in Fig. 1 for the H atom. Most known mesons are included in these plots. The omissions are 11 higher radial and angular excitations of non-strange light mesons, 5 higher radial excitations of strange mesons, 4 higher J/ψ states and 4 higher Υ states. The 9 known 'D' mesons with open charm and the 4 'B' mesons with open bottomness have also been omitted.

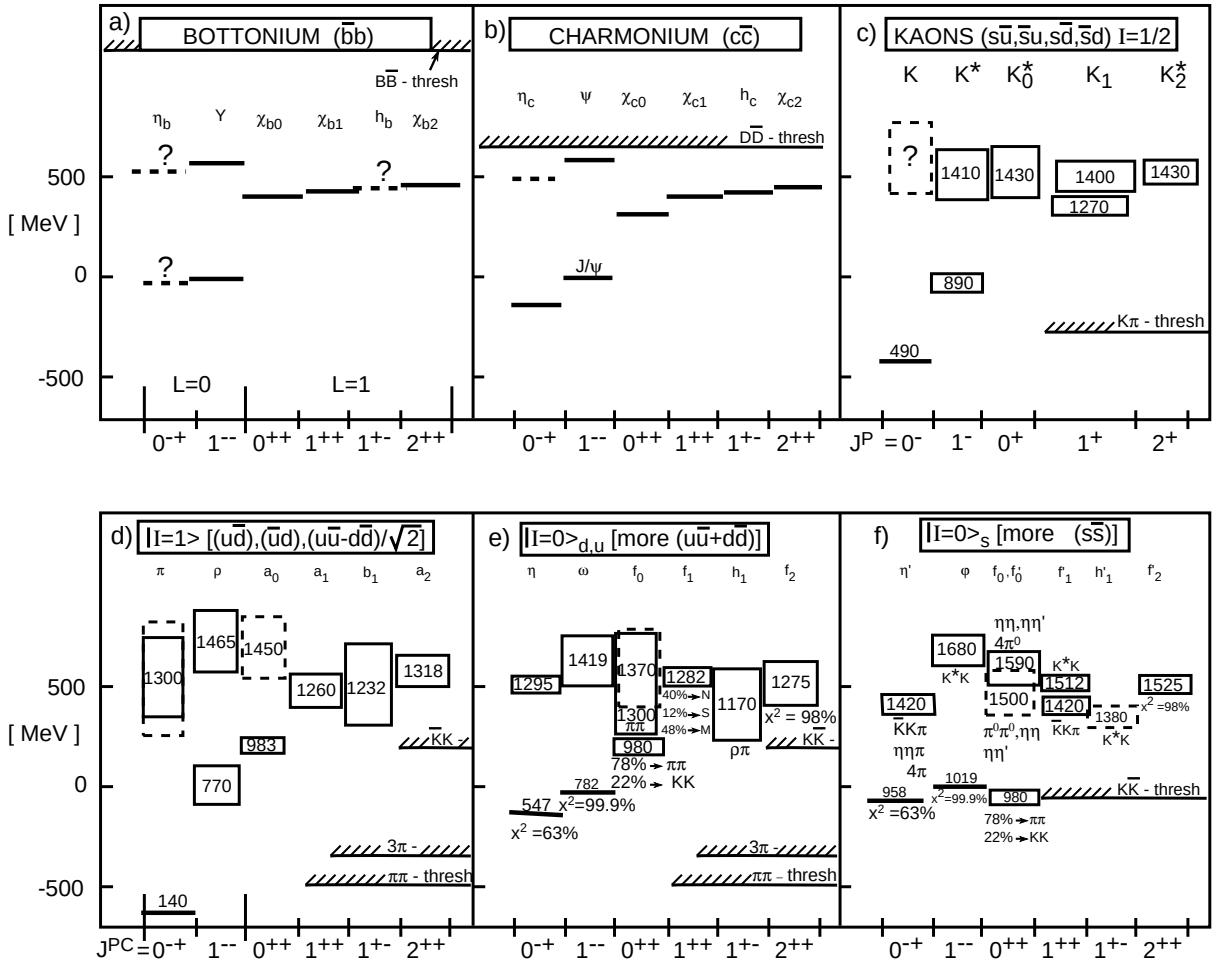

Figure 3: Level schemes of mesons, for $L \leq 1$ only, corresponding to the levels shown in Fig. 1. The vertical axis represents the energy difference to the 1^- ground state. This scale was chosen to facilitate a comparison of the level schemes of mesons with different total masses. The horizontal axis represents J^P or J^{PC}. The symbols for the different mesons are given under the figure titles for each J^{PC}. Each state is represented by a box or line, the height of which corresponds to the width Γ. The number in the box or above the line indicates the rest energy in MeV. a) Bottonium; b) charmonium; c) kaons (two isodoublets per box); d) isovectors (I = 1, a triplet of states per box). The isoscalars have been separated according to their dominant quark content. Those with more $\bar{u}u + \bar{d}d$ have been put in (e), those with more $\bar{s}s$ in (f). The fraction of the dominant component is indicated by $X^2 = ..\%$ if the nonet mixing angle is known. Otherwise the dominant decay modes are indicated. There are three exceptions to this rule of classification: the $f_0(980)$ has been assigned to both (e) and (f), and $f_0(1500)$ and $f_0(1590)$ have been put into (f) because the corresponding place in (e) was already too crowded. Based on the present knowledge of their decay modes, $f_0(1500)$ at least should be in (e); however perhaps it is not a normal meson.

Charmonium and bottonium (Fig. 3a and b) are eigenstates of the charge conjugation operator $\mathbf{C}$, hence can be characterized by the three quantum numbers J^{PC} (horizontal coordinate). The vertical coordinate is the energy of the state relative to the lowest state with $J^{PC} = 1^{--}$. All the displayed states are very narrow, i.e. have a long lifetime in comparison with most of the light mesons. This is one of the reasons why these

two-level schemes have found their way into high-energy physics textbooks more rapidly than the light mesons.

The reason for the long lifetime is described by the so-called OZI rule [4]. According to this rule, decays where $\bar{c}c$ and $\bar{b}b$ annihilate are suppressed compared to those decays where these quarks are transferred to the decay products. An example of an OZI forbidden decay is $\bar{c}c \to \bar{u}d + \bar{d}u$ (Fig. 4a).

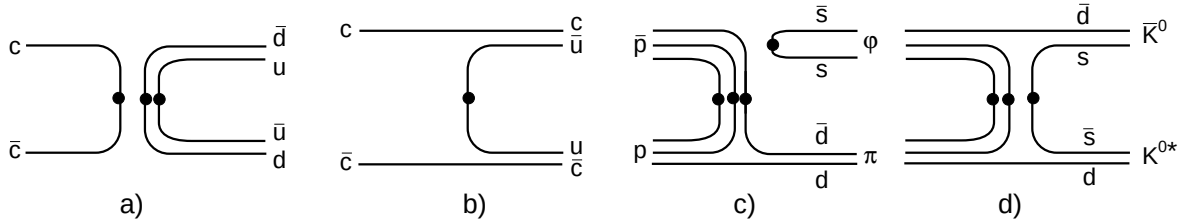

Figure 4: Examples of OZI forbidden and allowed processes: (a) forbidden decay of charmonium into non-charmed mesons; (b) allowed decay of charmonium into mesons with open charm; (c) forbidden ϕ meson production in $\bar{p}p$ annihilation; (d) allowed production of mesons with open strangeness.

An example of an OZI allowed decay is $\bar{c}c \to \bar{c}d + c\bar{d}$ (Fig. 4b). The OZI rule also applies to decays of $\bar{s}s$ pairs and to the inverse processes when heavy quark pairs ($\bar{s}s, \bar{c}c, \bar{b}b$) are produced (Fig. 4c and d). The thresholds for the OZI allowed decays to $D\bar{D}$ and $B\bar{B}$ are shown in Fig. 3.

Comparing with the H atom (Fig. 1), one notices — apart from the gigantic difference in the energy scales (a factor of 10^8) — that the splitting between S (L = 0) and P (L = 1) states is significant in both cases, and that the hyperfine splitting between η_c and J/ψ is large. A comparison of $\bar{c}c$ and $\bar{b}b$ shows that, in spite of the vastly different rest energies, 3097 MeV for J/ψ and 9460 MeV for $\Upsilon(1S)$, the energy separations between the levels are very similar, which is a remarkable fact.

The most prominent difference between the above level schemes and that of K mesons (Fig. 3c) is that, for the latter, all but one states are represented by boxes. The height of the boxes is equal to the width Γ of the resonance. Only the pseudoscalar ground state of the kaons cannot decay by strong interaction; it decays weakly. All others decay strongly and rapidly; there is no OZI suppression of the decay. The first radially-excited state with $J^P = 0^-$ has not yet been established with certainty. The hyperfine splitting between 0^- and 1^- ground states is 400 MeV, much larger than the corresponding splitting of the $\bar{c}c$ mesons. The first radial excitation of the 1^- and the P states appear as almost degenerate, at least relative to their widths. The gap between the 1^- ground state and its first radial excitation is 500 MeV, which seems to be a canonical number for **all** mesons. The K mesons are not eigenstates of **C**, therefore the states with $J^P = 1$ ($^1P_1$ and $^3P_1$) mix.

The isospin triplet states π, ρ, a_0, etc. are shown in Fig. 3d. Only the neutral member of each triplet is an eigenstate of **C**. The similarity of the energy gaps to the previous schemes is striking, apart from the hyperfine splitting between π and ρ, which is further increased compared to the previous cases. The $a_0(980)$ looks like an outsider because of its mass, width and decay branching ratios. It is discussed as a candidate for a $\bar{K}K$ molecule, together with the $f_0(980)$ which appears to be the I = 0 partner of this state. The scalar

state at 1450 MeV has been discovered only recently [5] and needs confirmation. It could be another candidate for the quark model ground state.

For the isoscalars shown in Fig. 3e and f, the mixing of the SU(3) singlet and octet states makes the identification of the two physical states even more difficult. (Moreover, if glueballs exist, additional states come in and mix.) If we take as a new basis for the two quark model states $|\bar{u}u + \bar{d}d\rangle/\sqrt{2}$ and $|\bar{s}s\rangle$, since we are interested in the $\bar{s}s$ component of mesons, the physical states are given by

$$|I = 0\rangle_{d,u} = X|\bar{u}u + \bar{d}d\rangle/\sqrt{2} + Y|\bar{s}s\rangle$$

$$|I = 0\rangle_{s} = -Y|\bar{u}u + \bar{d}d\rangle/\sqrt{2} + X|\bar{s}s\rangle$$

with $X^2 + Y^2 = 1$. Here X = $\cos(\theta - \theta_{\rm ideal})$, where θ is the conventional nonet mixing angle and $\theta_{\rm ideal}$ is the ideal conventional mixing angle of 35.3°. For $X > 0.5$ the state $|I = 0\rangle_{d,u}$ consists dominantly of $\bar{u}u + \bar{d}d$, and $|I = 0\rangle_{s}$ consists dominantly of $\bar{s}s$.

According to their dominant $\bar{q}q$ content, the mesons have been assigned to either (e) or (f) if the mixing angle is known (taking the average of the mixing angles obtained with the linear and quadratic mass formulae). If the mixing angle is not known, the meson is assigned to (e) if the decay is dominantly into non-strange mesons and otherwise into (f). The three exceptions are $f_0(980)$ which is displayed in (e) and (f), and $f_0(1500)$ and $f_0(1590)$, which are assigned to (f) for the sake of clarity.

3 DETECTING STRANGE MESONS AND HIDDEN STRANGENESS

How are mesons detected and how does one determine whether they contain $s, \bar{s}$ or $\bar{s}s$? This will be our next subject. I shall first describe the basic features of a modern detector for meson spectroscopy (of course, this will be the one I am involved with). I will then describe how stable strange mesons, unstable strange mesons and mesons with $\bar{s}s$ content are identified with this detector. First of all it is necessary that we understand the time and space evolution of events in which mesons are produced and detected.

3.1 Space–time evolution of events

As an example, let us consider $\bar{p}p$ annihilation. This is a process which is especially well suited to meson spectroscopy. When a $\bar{p}$ annihilates at rest, practically only mesons are produced. Among them, exotic mesons (gluonia, hybrids, etc.) are expected.

An interesting sequence of events takes place even before the annihilation. The antiproton, slowed down in the target, is caught by an H_2 molecule in some high atomic orbit, ejecting an electron if the binding energy of the $\bar{p}$ is larger than that of the electron. From the ratio of reduced masses of the $\bar{p}p$ atom and electron, the initial main quantum number can be estimated to be around 30. After formation, the $\bar{p}p$ atom is de-exited by radiation and the Auger effect until $\bar{p}$ and p have approached close enough to each other for the strong force (range of about a femtometre) to start acting.

What are the **elementary QCD processes** that take place at annihilation? The incoming $\bar{p}$ consists of three valence antiquarks and of sea quarks and gluons; the p consists of 3 valence quarks, sea quarks and gluons. The elementary processes are (Fig. 5)

- rearrangement of quarks and antiquarks into pairs (mesons);
- fusion of a quark with the corresponding antiquark into a gluon, and the reverse process — dissociation of a gluon into a $\bar{q}q$ pair;
- dissociation of a gluon into two gluons, and the reverse process — the fusion of two gluons into one;

– scattering of two gluons (4-gluon vertex).

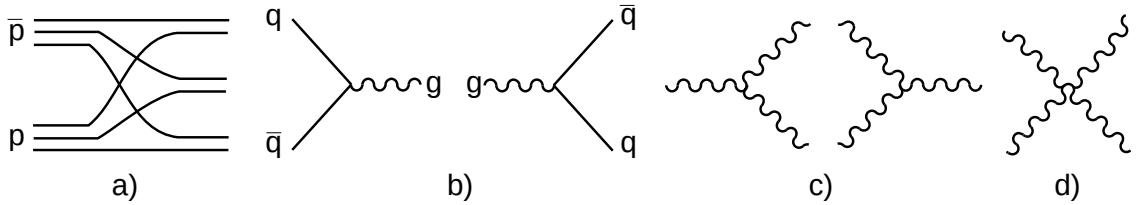

Figure 5: QCD processes taking place in $\bar{p}p$ annihilation: (a) rearrangement, (b) fusion and pair creation, (c) gluon dissociation, (d) 4-gluon vertex.

It is obvious that by appropriate combination of these processes, normal meson states, gluonia, 4-quark states or hybrids can be formed. These processes are confined in hadrons and take very short times, of the order of 10^{-24} s. The lifetimes of the hadrons emerging from the interaction vary from 10^{-24} to 5×10^{-8} s. Consider a specific example, the annihilation

$$\bar{p}p \rightarrow K^{+*}K^{-},$$

which implies the fusion of an incoming $\bar{u}u$ and a $\bar{d}d$ pair and the creation of an $\bar{s}s$ pair:

$$\bar{u}\bar{u}\bar{d} + uud \rightarrow u\bar{s} + \bar{u}s \quad .$$

The K^{+*} decays with a lifetime $\tau = \hbar/\Gamma$ of about 10^{-23} s into $K\pi$, i.e. either $K^{+}\pi^{0}$ or $K^{0}\pi^{+}$. In the laboratory, due to time dilation, the distance the K^{+*} traverses before it decays (its decay path) is

$$\tau \cdot \gamma \cdot v = c\tau \cdot pc/(mc^2) \quad ,$$

where $\gamma = (1-\beta^2)^{-1/2}$, with $\beta = v/c$, $v =$ the velocity, $p =$ the momentum, $mc^2 =$ the rest energy of K^{+*}. For a typical momentum of around 500 MeV/c the decay path is 3 fm — short indeed! Due to its short lifetime the state $K^{+*}K^{-}$ is called an **intermediate state.**

Let us assume that after the decay of the K^{+*} we have the three particles K^{+} and $\pi^{0}K^{-}$. This state is called the **'final' (hadron) state**, although it is only final with respect to the hadrons. The final hadrons decay due to the action of weak and electromagnetic forces. The π^{0} decays electromagnetically in 8.4×10^{-17} s, mainly (99%) into two photons, 2γ. The corresponding decay path is still very short, some tens of nanometres. The K^{+} and K^{-} decay weakly, most frequently into $\mu\nu$ or $\pi\pi$; and the charged pions decay into $\mu\nu$. Finally, the μ's decay into $e^{\pm}$ and a pair of ν's. The relevant lifetimes τ and the products $c\tau$ are listed in Table 3.

Table 3: Lifetimes (τ) and products ($c\tau$)

	K^{*}	π^{0}	K_S	K_L	$K^{\pm}$	$\pi^{\pm}$	$\mu^{\pm}$
τ [s]	10^{-23}	8.4×10^{-17}	8.9×10^{-11}	5.2×10^{-8}	1.2×10^{-8}	2.6×10^{-8}	2.2×10^{-6}
$c\tau$ [m]	3×10^{-15}	2.5×10^{-8}	2.7×10^{-2}	15.5	3.7	7.8	659

The decay paths of the weakly decaying particles are several metres long or more. The truly final, truly stable particles are the photons, electrons or positrons and neutrinos.

In vacuo they would live forever. In the real world they interact; this is how they are detected (it is difficult to detect the interaction of neutrinos but possible).

Our presumed detector, about 2 m in diameter, will intercept the sequence of events before 10^{-8} seconds have passed, i.e. the π^0 has decayed but K^+ and K^- are still alive. Hence these are the detected particles in this special event. In the general case of $\bar{p}p$ interaction at rest, the detector has to detect π^+ and π^- in addition to γ, K^+ and K^-.

3.2 Detecting strange mesons and $\bar{s}s$ components

It is now easy to understand how (openly) strange mesons, i.e. those containing one s or $\bar{s}$ quark, are detected. Since strangeness is conserved in strong interactions, the strange quark has to be found in the decay products. There has to be a K^+, K^-, K^0 or $\bar{K}^0$ in the final hadron state. If a meson resonance is found to decay into an odd number of K mesons, it must be strange.

Because strangeness is conserved in strong interactions and the initial state has S = 0, even numbers of Ks, i.e. $\bar{K}K$ pairs, are always observed in $\bar{p}p$ annihilation. They can come from three sources:

(i) a pair of strange mesons in the intermediate state;
(ii) a meson with hidden strangeness;
(iii) a meson without any strange quark constituent where $\bar{s}s$ is created in the decay.

An example for a prediction from flavour SU(3), relevant to sources (ii) and (iii), is given below.

If $f_0 = (\bar{u}u + \bar{d}d)/\sqrt{2}$ then $BR(f_0 \to \bar{K}K)/BR(f_0 \to \pi\pi) = 1/6$;
if $f_0' = (\bar{s}s)$ then $BR(f_0' \to \bar{K}K)/BR(f_0' \to \pi\pi) = 1/0$;
if $f_0 =$ glueball then $BR(f_0 \to \bar{K}K)/BR(f_0 \to \pi\pi) = 4/3$;
if $f_0 =$ meson-antimeson $(M\bar{M})$ molecule, then $BR(f_0 \to M\bar{M})$ is dominant.

3.3 A modern detector — the Crystal Barrel spectrometer

The detector is required to detect photons, charged kaons and charged pions, and to measure their momenta and angles for momenta up to about 2 GeV/c. In order to detect all particles produced in an event, it has to cover the complete solid angle 4π sr, or at least a big fraction of it. Figure 6 shows how this is achieved with the Crystal Barrel detector at LEAR (the Low Energy Antiproton Ring at CERN). The $\bar{p}$ beam from LEAR enters from the left, along the z axis. This beam is the best antiproton beam in the world, with the following characteristics, compared to the values for a conventional $\bar{p}$ beam, such as at BNL (USA) or KEK (Japan), in brackets. Intensity: 10^4–10^7 $\bar{p}/s$ ($< 10^5$ $\bar{p}/s$); momentum resolution: $\Delta p/p = 10^{-3}(3 \times 10^{-2})$; purity: 100% $\bar{p}$(1% $\bar{p}$); beam cross-section: 1 mm^2 (5 cm^2).

The beam is stopped or interacts in flight in a tiny target containing liquid or gaseous H_2 or D_2. The target can be so small because of the beam quality. A tiny target is a big advantage: precise definition of the primary interaction vertex, few secondary interactions in the target, close approach of detectors to the point of interaction. The target is surrounded by a 2-layer multi-wire proportional chamber (PWC) or, more recently, by a silicon microstrip vertex detector (SVX). The PWC or SVX is surrounded by a cylindrical Jet Drift Chamber (JDC) with 23 layers of wires and 30 azimuthal sectors. The JDC is located inside a cylindrical photon calorimeter consisting of 1380 Cs(Tl) crystals, each 30 cm long. This crystal barrel gave its name to the whole spectrometer. All the active detectors are embedded in a solenoidal magnet which produces a homogeneous axial field

(parallel to the cylinder, beam or z axis) of strength 1.5 T. The detector is described in detail in a long paper [6]. Here we only want to outline the particle detection methods with this apparatus.

With the JDC, charged tracks are measured at up to 23 space points. The wires are parallel to the z axis. Thus, each drift time provides precise information on r (distance of the wire to the beam axis) and ϕ (azimuthal angle). The left–right ambiguity is solved by staggering the wires. The spatial resolution (σ) in the r–ϕ plane is about 100 μm for each point. A measurement of the z coordinate is provided by charge division: the sense wires have a suitable resistance and the signal is read out on both sides of the wire. From the charge ratio, the z location of the track can be determined with a precision (σ) of 5 mm. The total charge is proportional to the energy loss of the particle in the chamber ($\mathrm{d}E/\mathrm{d}x$). This energy loss is useful to distinguish between $K^{\pm}$ and $\pi^{\pm}$. Since the tracks are curved in the magnetic field [$pc/\mathrm{MeV} = 300 \cdot (B/Tesla)(\rho/m)$, where ρ/m is the radius of the orbit in metres for $\vec{p}$ orthogonal $\vec{B}$], the momentum can be measured with a precision (σ) of between 2% and 6% for momenta p_T between 0.1 and 1 GeV/c (p_T is the momentum component orthogonal to z).

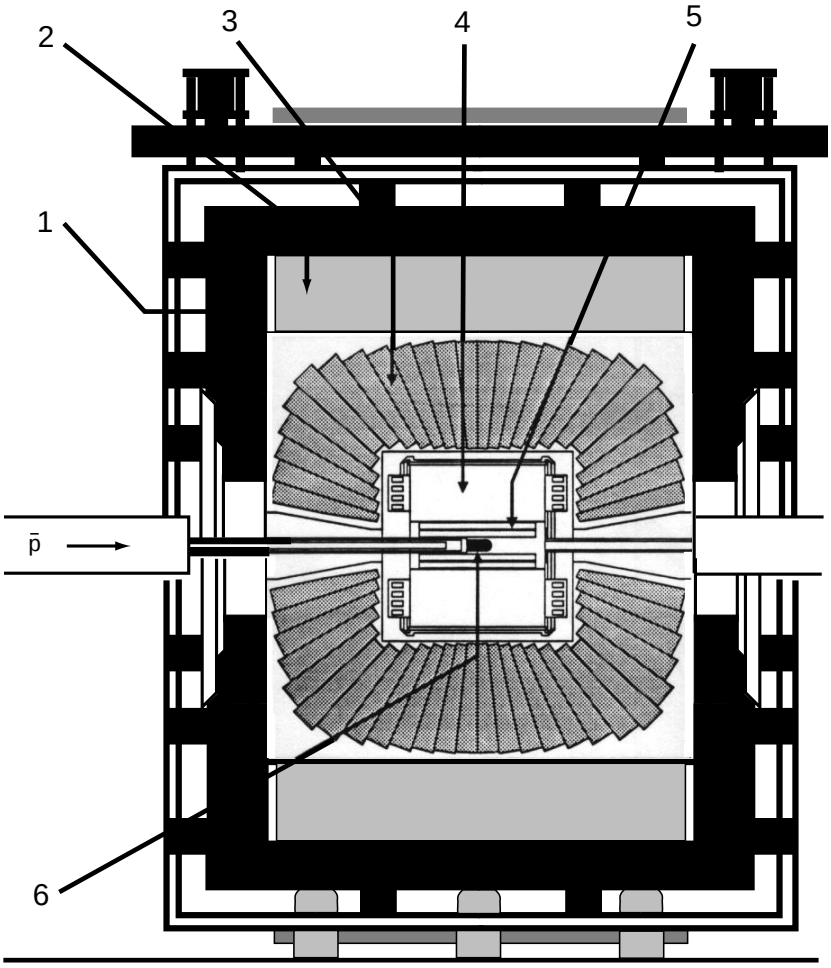

Figure 6: The Crystal Barrel spectrometer at LEAR cut along the cylinder symmetry axis (z axis). Components: (1) magnet yoke, (2) magnet coil, (3) electromagnetic calorimeter, (4) jet drift chamber, (5) proportional chamber and (6) target.

The main role of the PWC or SVX is to provide a fast trigger on the multiplicity

of charged particles in the final state. For instance, if one wants to record only events in which no charged particle emerges from the target, PWC or SVX are used as veto counters and events are rejected if a charged particle is detected. In combination with the requirement of observing charged tracks, this can be used to set up a powerful trigger for events with strange particles, see below.

The CsI(Tl) crystals of the calorimeter are read out by photodiodes via a wavelength shifter. Inorganic crystals are the best but also most expensive material for detecting high-energy photons. The granularity of the calorimeter has been chosen such that for the given distance to the target optimal angular resolution and shower separation are achieved. Each high-energy photon induces an electromagnetic shower (a cascade driven by pair production and bremsstrahlung, which involves thousands of photons and electrons). Each shower is distributed in general over several crystals. From the centre of gravity, the impact point of the primary photon is determined. The energy resolution of the calorimeter for photons is

$$\sigma_E/E = 2.5\%(E/\mathrm{GeV})^{-1/4}.$$

Great care has been taken to minimize the electronic noise in the read-out of the crystals in order to be able to extend the measurement to the lowest possible energy. The noise of the crystals corresponds to less than 300 keV. However, the lowest reasonable energy threshold is 5 MeV. At these low energies 'physical' noise (statistical shower fluctuations which seem to come from separated showers) becomes dominant. These fluctuations are called 'split-offs'. The collaboration has learnt progressively how to recognize split-offs, employing neural networks among other techniques in order to improve the calorimetry in the low-energy region.

3.4 Detecting stable mesons

The weakly-decaying charged kaons and pions live long enough that they decay outside our detector, which occupies a cylinder of 1.5 m diameter and 1.5 m length. Together with the long-lived neutral K meson (the K_L to be discussed below) they are the only neutral mesons with such long lifetimes.

How are the charged kaons detected? First, their momentum is measured in the JDC. In many cases, this is enough to identify them, i.e. to distinguish them from the other charged mesons (the pions). Take for example the annihilation into two charged stable mesons,

$$\bar{p}p \to K^+K^-, \quad \bar{p}p \to \pi^+\pi^- \quad .$$

The particles are monoenergetic, their momentum is determined by energy and momentum conservation and related to the mass of the particles produced (Fig. 7a).

If there are more than two particles in the final state, and if one wants to distinguish for instance between the two reactions $\bar{p}p \to K^+K^-\pi^0$ and $\bar{p}p \to \pi^+\pi^-\pi^0$, energy and momentum conservation in general allow this to be achieved, although the particle momenta vary. This is done in the kinematic fit. (The higher the precision of energy and momentum measurement, the clearer the distinction.)

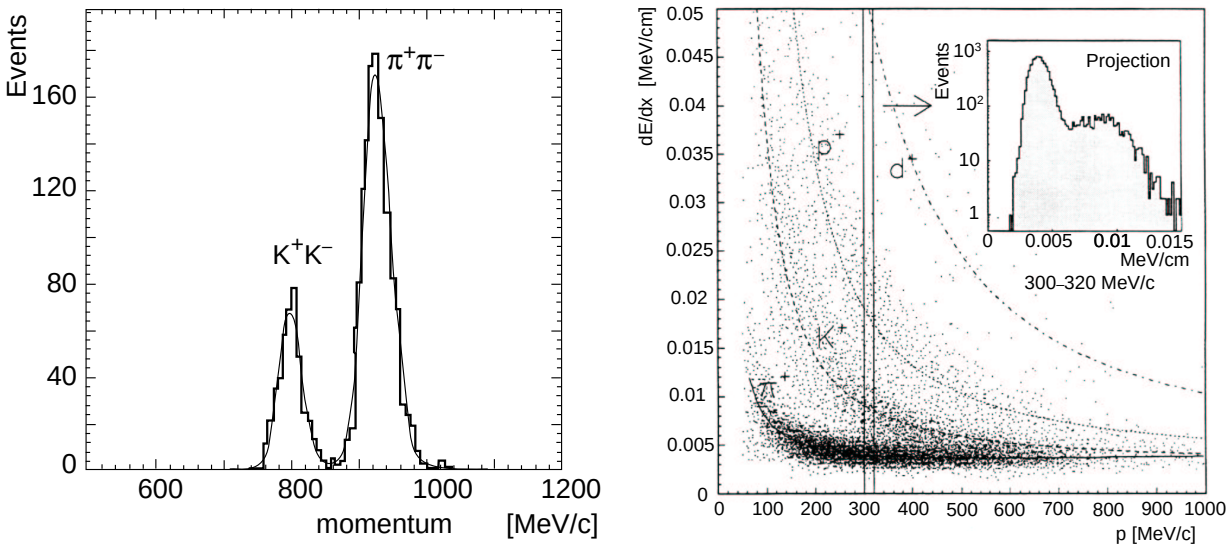

Figure 7: a) Momentum distribution of particles in colinear two-prong events due to the reactions $\bar{p}p \to K^+K^-, \bar{p}p \to \pi^+\pi^-$; (b) energy loss versus momentum for charged tracks, measured in two-track events with two to four additional showers in the calorimeter (from a study of $\bar{p}p \to K_L K^{\pm}\pi^{\mp}\pi^0$, C. Kolo, thesis, University of Munich 1995).

The additional tools for distinguishing between kaons and pions are in general, measurement of time of flight, Cherenkov radiation and energy loss $\mathrm{d}E/\mathrm{d}x$. All these measurements provide information on the velocity v of the particle which, combined with the momentum $p = mv$, fixes m. Figure 7b shows a $\mathrm{d}E/\mathrm{d}x$ measurement in the JDC of the Crystal Barrel detector as a function of momentum. The bands which can be seen are associated with π's and Ks (and p's and d's from secondary interactions). The separation is good for momenta up to 400 MeV/c.

3.5 Less stable mesons

Neutral π^0 , η and η' mesons have very long lifetimes on the scale of strong interactions, but decay practically at the primary interaction vertex. These particles are identified through their decay products. All of them have a decay mode into two photons, with the following branching ratios: 99% for π^0, 39% for η, 2% for η'.

They are identified by calculating the invariant mass $M_{\gamma\gamma}$ of any pair of γ's produced in the event,

$$M_{\gamma\gamma} = \sqrt{(p_1 + p_2)^2} \quad ,$$

where p_1 and p_2 are the 4-momenta of the two photons. This invariant mass is equal to the mass of the mesons within the measurement errors expected if the two γ's were indeed the decay products (Fig. 8) [6].

In the sort of event used for Fig. 8 there were 6 photons and hence 15 possible pairs. Assuming that all photons come from either one of the possible 3-meson final states ($\pi^0\pi^0\pi^0$, $\pi^0\pi^0\eta$, $\pi^0\eta\eta$, $\pi^0\pi^0\eta'$, etc.), there are only three good combinations for each event. The remaining 12 wrong combinations are called combinatorial background. This usually flat background sits under the signal peaks. Since a photon pair is associated with a meson if the invariant mass falls within an appropriate window containing the signal peak, it is obvious that a smaller window implies a smaller contribution from the combinatorial background. This is why good energy and momentum resolution of the

detector is a definite advantage. The better the mass resolution, the cleaner the selected sample of events.

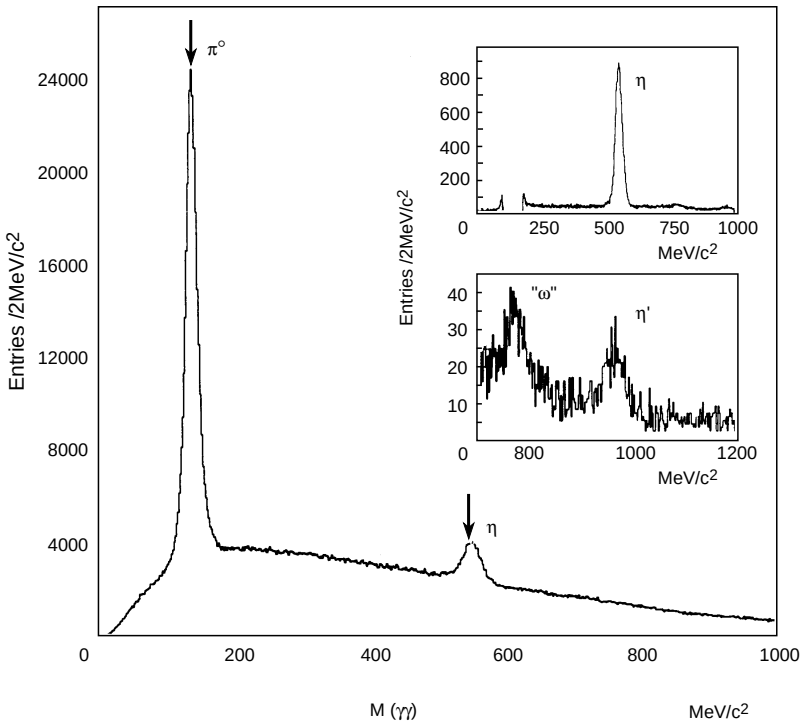

Figure 8: Invariant mass distribution of two photons, $M_{\gamma\gamma}$, for 6 photon final states in $\bar{p}p$ annihilation at rest ($\bar{p}p \to 6\gamma$). The insests show the mass distribution after pairs of γ's have been removed which fall into the π^0 window (upper inset) and into the π^0 or η window (lower inset).

The figures of merit of the Crystal Barrel detector for the mass resolution of π^0, η, η' in 6-photon events are

$$\sigma_{\pi^0} = 10 \text{ MeV} , \quad \sigma_\eta = 16 \text{ MeV} , \quad \sigma_{\eta'} = 17 \text{ MeV} .$$

Other decay modes can also be used to identify these particles (e.g. $\eta \to 3\pi^0$) by calculating the invariant mass of all the particles produced in the decay.

In the latter case

$$M = \sqrt{(p_1 + p_2 + p_3)^2} .$$

In Fig. 8 a signal called ω can be seen. The ω decays 8% into $\pi^0\gamma$ and is frequently produced in the reaction

$$\bar{p}p \to \pi^0\pi^0\omega .$$

It is background from this channel which is seen in Fig. 8. Suppose a very low-energy γ is lost from the decay of the ω, such that the loss is not noticed by the requirement of energy and momentum conservation. The event will only have 6 photons and the invariant mass of the remaining two photons from the ω decay will be almost correct. This is the origin of the signal in Fig. 8 and it demonstrates again the importance of good momentum and energy resolution and a low energy threshold for detecting photons in this kind of physics.

3.6 Neutral K mesons

The neutral K mesons are very special in many respects. They are described in all particle physics books. A superb chapter of the Feynman lectures (Vol. 3) is dedicated to them; it was even written before the discovery of CP violation, which added another exciting chapter to neutral K physics.

For the present context of detecting kaons, it is important to realize that the particles observed are not K^0 or $\bar{K}^0$, the eigenstates of the strong interaction, but K_L and K_S, which are introduced in textbooks as the two eigenstates of **CP** with the eigenvalues CP $= \pm 1$, plus some small CP-violating admixtures of the eigenstate of opposite CP. Ignoring these small admixtures, which lead to barely any observable effects in meson spectroscopy, we may consider them as CP eigenstates and as eigenstates of C and P, separately, with respect to the strong interaction. With $\mathbf{C}K^0 = -\bar{K}^0$, $\mathbf{C}\bar{K}^0 = -K^0$ (see Appendix), $\mathbf{P}K^0 = -K^0$ and $\mathbf{P}\bar{K}^0 = -\bar{K}^0$ (pseudoscalars, i.e. P= –1) the eigenstates are

$$K_S \approx K_1 = (K^0 + \bar{K}^0)/\sqrt{2}; \qquad CP = +1, \;\; C = -1$$

$$K_L \approx K_2 = (K^0 - \bar{K}^0)/\sqrt{2}; \qquad CP = -1, \;\; C = +1 \;\; .$$

The lifetime of the K_S is such that it decays a few centimetres from the vertex (see Table 3). This is normally within the detector but well away from the primary interaction vertex. The secondary interaction vertex provided a powerful tag to identify K_S in bubble chambers many years ago. It can also be used in electronic counter experiments to provide a trigger on events with a K_S. This is an interesting possibility since these events are relatively rare, and enhancement by a specific trigger is in general required to obtain samples with a high number of events for final states which are rare. The dominant decays of the K_S are

$$K_S \to \pi^+\pi^-, \qquad K_S \to \pi^0\pi^0 \;\; .$$

The K_S is identified by calculating the invariant mass of the two pions (see Fig. 9).

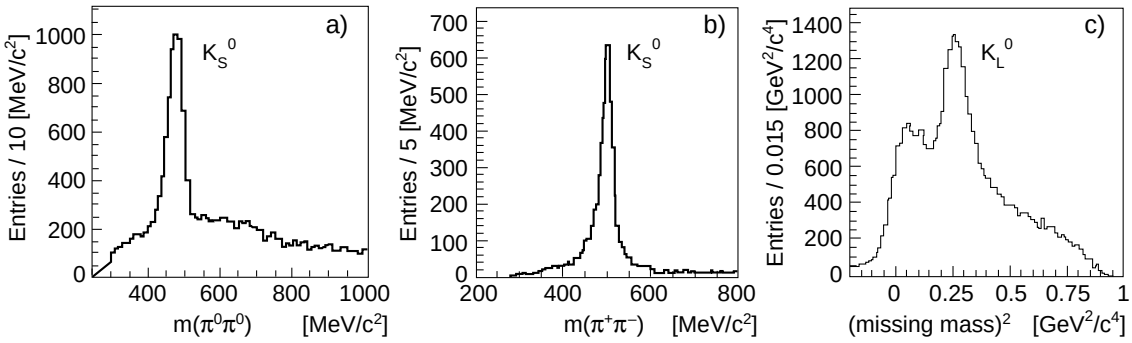

Figure 9: Identification of K_S via its decay into two charged or neutral pions. Invariant mass distributions of (a) $\pi^0\pi^0$ from an analysis of the reaction $\bar{p}p \to K_S K_L \pi^0$; (b) of $\pi^+\pi^-$ from an analysis of the reaction $\bar{p}p \to K_S K_S \pi^0$ with one K_S decaying into $2\pi^0$, the other one into $\pi^+\pi^-$; (c) identification of K_L's by the missing mass technique. (Thesis of H.P. Dietz, University Munich 1994.)

The charged decay mode is used to trigger on events with a K_S. The trigger of the Crystal Barrel spectrometer requires simply that in the JDC two additional tracks are detected compared to the SVX (or PWC before it was replaced by the SVX). The PWC

had a radius of 2.6 cm, the SVX has a radius of 1.2 cm. The smaller radius of the SVX significantly improves the trigger efficiency at lower K_S momenta (100–200 MeV/c).

The lifetime of the K_L and its decay path are so long (Table 3) that it usually decays outside the detector. Since it is neutral it is not seen in the tracking chambers, but there is a 50% chance that it interacts in the crystal calorimeter. These properties of the K_L can be used to identify it, as long as all the other particles in the final state are detected. For this purpose, the detector has to be hermetic, i.e. cover 4π sr. If the K_L has not interacted, the missing mass

$$M_{\rm miss} = \sqrt{(p_{\rm miss})^2} = \sqrt{(E^2_{\rm miss} - \vec{p}^2_{\rm miss})}$$

can be calculated from missing energy and momentum, $(E_{\rm miss}, \vec{p}_{\rm miss})$, i.e. the differences between the sum of detected particle energies and momenta and the incoming energy and momentum (Fig. 9b). If it has interacted, the energy deposit in the crystals does not provide any good information on the energy of the K_L, since the fluctuations of such hadronic showers are very large; however, the information on the angle is still useful. This technique allows identification of events of the type

$$\bar{p}p \rightarrow K_L K_L \pi^0$$

and determination of their complete kinematics.

3.7 Short-lived states

Short-lived states, also called resonances (between the hadrons into which they decay), are in principle detected, like 'stable' hadrons, by calculating the invariant mass of the decay products. Whereas the width of a stable or very narrow resonance is usually determined by the detector resolution, broad resonances have a natural width which is much larger than the detector resolution.

Detecting and identifying resonances is, in general, much more difficult if they are broad than if they are narrow. In many cases, there is even justification in saying that for the hunters of short-lived hadrons the real data analysis work begins where it ends for other particle physicists. After selection of the final state and subtraction of the background (this is the point where the normal particle physicist is ready to publish the observation of a signal or an upper limit) an **amplitude analysis** has to be performed, which can be very tedious. The main reason for the difficulty is that short-lived resonances, since they are broad, very rarely 'stand alone' but rather overlap and interfere with each other.

Let us first consider the hypothetical production of an isolated resonance in $\bar{p}p$ annihilation (Fig. 10).

In order to form a resonance in production, the final state has to contain at least three particles and the total energy $\sqrt{s_{\bar{p}p}} = M_{\bar{p}p} = \sqrt{(p_{\bar{p}} + p_p)^2}$, i.e. the available phase space, must be sufficiently large. The case of 3 particles is of course the simplest. Such a final state can be described by two kinematic variables if we assume that there is no preferred direction, as is the case for the annihilation of unpolarized $\bar{p}p$ at rest. The usual variables are the invariant masses squared between pairs of particles, for instance

$$m_{12}^2 \equiv s_{12} = (p_1 + p_2)^2$$
$$m_{13}^2 \equiv s_{13} = (p_1 + p_3)^2 \quad ,$$

where the p_i are the 4-vectors.

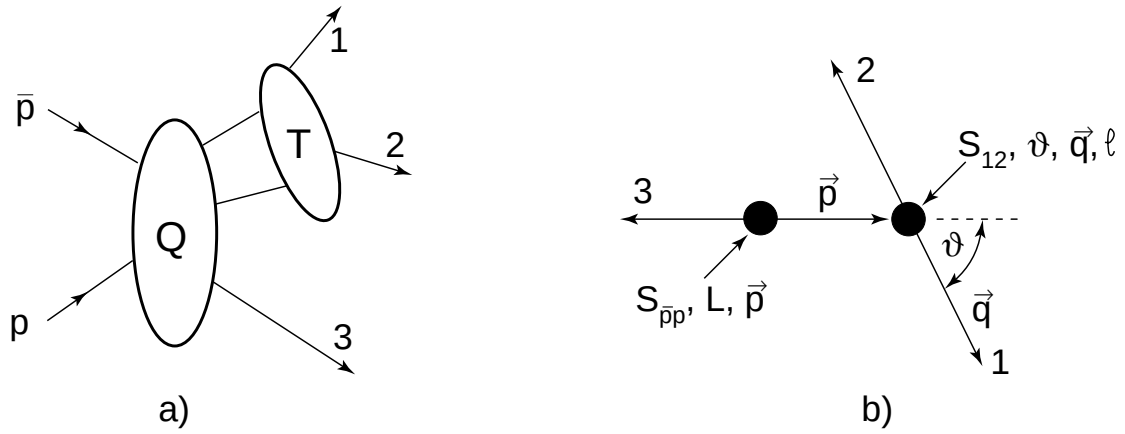

Figure 10: (a) Production of a 3-body final state in $\bar{p}p$ annihilation with a resonance between particles 1 and 2; (b) definition of the corresponding kinematic variables s_{12}, s_{13} (invariants), $\vec{p}$ and L (defined in the $\bar{p}p$ cm system), and $\vec{q}, \theta$ (defined in the rest system of the resonance the Gottfried–Jackson system, see text).

The third invariant mass is then given by the relation

$$s_{12} + s_{23} + s_{13} = s_{\bar{p}p} + s_1 + s_2 + s_3 \quad ,$$

where $s_i \equiv m_i^2$. Each event can be represented by a point in the plane s_{13} versus s_{12}, and the collection of points (scattergram) corresponding to a sample of many events is called a **Dalitz plot**. It can be shown that a homogeneous distribution of points corresponds to a homogeneous phase-space distribution of the final-state particles.

Now suppose that only one initial $\bar{p}p$ state with quantum numbers J^{PC} contributes and only particles 1 and 2 resonate with angular momentum l. Assuming for simplicity that all three final-state particles are (pseudo)scalars, l equals the spin of the resonance. Then the observed intensity (normalized density of points in the Dalitz plot) is

$$I(s_{12}, s_{13}) = \mid \sum A_{JPC,L,l}(s_{12}, s_{13}) \mid^2 \quad ,$$

where the sum $\sum$ runs over L, the possible angular momenta between particle 3 and the resonance. The total amplitude is a (coherent) sum over L since, in general, different L may combine with a fixed l to the same J. The partial amplitude $A_{JPC,L,l}$ is given by the following product:

$$A_{JPC,L,l}(s_{12}, s_{13}) = Z_{JPC,L,l}(\vec{p}/p, \vec{q}/q) D_L(p) F_l(q) \quad ,$$

where $\vec{p}/p$ is the direction of the resonance in the laboratory and $\vec{q}/q$ is the direction of particle 1 relative to the $\vec{p}$ after a Lorentz boost into the rest sytem of the resonance (Gottfried–Jackson system), see Fig. 10.

The momenta p and q are given in terms of s_{12}, s_{13} by

$$p^2 = [s_{\bar{p}p} - (m_{12} + m_3)^2][s_{\bar{p}p} - (m_{12} - m_3)^2]/4s_{\bar{p}p} \quad ,$$

$$q^2 = [s_{12} - (m_1 + m_2)^2][s_{12} - (m_1 - m_2)^2]/4s_{12} \quad .$$

The angle θ (Fig. 10) between $\vec{p}$ and $\vec{q}$ is given by

$$2s_{13} = [(s_{13})_{\max} + (s_{13})_{\min}] + [(s_{13})_{\max} - (s_{13})_{\min}] \cos\theta \quad ,$$

where $(s_{13})_{\min,\max}$ depend on s_{12}. The function $Z_{JPC,L,l}(\vec{p}/p, \vec{q}/q)$ is the spin-parity amplitude describing the angular correlations between the final-state particles due to angular momentum conservation. We have used notations which are customary when the non-relativistic Zemach formalism [7] is applied. Other formalisms are in use: the helicity formalism [8] and the Rarita–Schwinger formalism [9]. Recently, covariant formulations of the two former methods have been advocated [10, 11]. The spin-parity function Z seems to depend on more variables than s_{12}, s_{13}; however, when the sum of partial amplitudes is squared, the squares or mixed products of the Z functions (which are in reality tensors) are reduced to scalar functions of the angle θ. The function $D_L(p)$ is the 'angular momentum barrier' or 'penetration factor', taken to be proportional to p^L or a more complicated expression acccording to Blatt–Weisskopf [12]; and the factor $F_l(q)$, the 'dynamic function', describes the dynamics. For the case of a single isolated resonance it is given by the relativistic Breit–Wigner amplitude [13]

$$F_l = g^2/(m_0^2 - s_{12} - i\rho g^2)$$

with $\rho = 2q/\sqrt{s_{12}}$, m_0 the nominal resonance mass and $g^2 = m_0\Gamma_0 D_l(q)^2/\rho$.

The process leading to the production of the resonance may be conceptually factorized into two: first, the production of the three-body final state — described by the Q blob in Fig. 10a — and second, by the resonance or, more generally, final-state interaction between particles 1 and 2, described by the T blob in Fig. 10a. Thus this production process can be related to a different kind of process, the scattering of particle 1 on particle 2, described by the scattering amplitude T. If the scattering can be inelastic (i.e. in addition to the elastic scattering, e.g. $\pi\pi \to \pi\pi$, other final states are possible at the energy $\sqrt{s_{12}}$, e.g. $\pi\pi \to K\bar{K}$) then T has to be extended to be a matrix, the 'T-matrix'. For our example with two possible channels, T_{11} and T_{22} describe the elastic scattering $\pi\pi \to \pi\pi$ and $K\bar{K} \to K\bar{K}$, respectively, and T_{12} and T_{21} describe the transitions $\pi\pi \to K\bar{K}$ and $K\bar{K} \to \pi\pi$, respectively. The factor Q turns into a vector, the 'Q-vector', where Q_1 describes the production $\bar{p}p \to \pi\pi$ + spectator and Q_2 the production $\bar{p}p \to K\bar{K}$ + spectator. In our example, two diagrams contribute to the final state, with the intermediate particles 1 and 2 between the Q and T blobs being $\pi\pi$ or $K\bar{K}$.

We have outlined here the Q-vector approach [14] to the production. Other descriptions — the P-vector approach [15] (see, for example, [16]) or the N/D method (see, for example, [17]) — are being used to describe the production of resonances which couple to more than one continuum state. So far, we have made the simplifying assumption that only one resonance is being produced between 1 and 2. However, there may be more than one resonance between 1 and 2, with different l, and there may also be resonances, or more generally, final-state interactions between 1 and 3 and 2 and 3 and even between all three particles (like the rescattering of one of the decay products of the resonance on the spectator, which of course can then no longer be called the spectator). Usually, the

interactions involving three particles are ignored and it is assumed that the intermediate state always consists of a resonance and a stable hadron (the spectator or 'bachelor'), which do not interact (**isobar model**). Extending this model to final states with more than three particles, it is assumed that these states are reached by this kind of sequence, e.g. two resonances are produced which then in turn decay into two resonances and so on. All these amplitudes interfere with each other as long as they involve the same initial state and overlap in phase space, which is more likely for broader resonances. (If different initial states are involved, the corresponding intensities are added incoherently.) For instance, in one of the examples given above, the annihilation

$$\bar{p}p \rightarrow K^{+*}K^{-} \rightarrow (K^{+}\pi^{0})K^{-} \quad ,$$

the same final state can also be reached by annihilation via different intermediate states,

$$\bar{p}p \rightarrow K^{+}K^{-*} \rightarrow K^{+}(\pi^{0}K^{-}) \qquad \text{or} \qquad \bar{p}p \rightarrow \phi\pi^{0} \rightarrow (K^{+}K^{-})\pi^{0} \quad ,$$

from the same initial state. The brackets signify a resonance between the final-state particles within them. As in the 'classic' 2-slit experiment of quantum mechanics, the corresponding three amplitudes have to be added coherently.

Thus the sum over L in the expression above for the intensity has to be extended to a sum over various l, L and over all permutations of particles in order to also include resonances of other pairs of particles. Taking this extended sum, phase correlations following from symmetries should be respected. If, for instance, 1 and 2 are identical bosons, the sum of amplitudes has to be symmetrical with respect to the interchange of particles 1 and 2 (this automatically eliminates all odd angular momenta l in our example). If the final state is an eigenstate of C or G, various terms contributing to the total amplitude are connected by plus or minus signs (relative phase of 0 or 180°). For the case of states with $\bar{K}K$ pairs these eigenfunctions are derived and explicitly listed in the Appendix, since they are relevant for the search for mesons with open or hidden strangeness.

In Fig. 11 a series of four Dalitz plots for $\bar{K}K\pi$ final states with different charge combinations are shown as examples. The possible quantum numbers of the $\bar{K}K$ resonances are listed in Table 4.

Table 4: Quantum numbers of $\bar{K}K$ resonances.

$\bar{K}K$	C	Isospin	J^{PC}	Possible resonances
K_LK_S	−1	0,1	1^{--}	ϕ
K_LK_L, K_SK_S	1	0,1	$0^{++}, 2^{++}$	a_0, f_0, a_2, f_2
$K_LK^{\pm}, K_SK^{\pm}$		1	$0^{+}, 1^{-}, 2^{+}$	$a_0, a_2, \rho, ..$
$K^{+}K^{-}$	± 1	0,1	$0^{++}, 1^{--}, ..$	$\phi, a_0, f_0, a_2, f_2, ..$

Our first example (Fig. 11a) from the reaction

$$\bar{p}p \rightarrow K_LK_S\pi^{0}$$

is a particularly simple one since only a few resonances occur. Remember that if no resonances at all occurred and the events were homogeneously distributed over the available phase space, the density of points in this Dalitz plot would be homogeneous within the kinematic boundaries. Resonances show up as vertical and horizontal bands for $K_L\pi^{0}$ and $K_S\pi^{0}$ and as anti-diagonal bands for the third pair of particles, K_LK_S. Fig. 11a

shows exactly one resonance for each case: a vertical and a horizontal band due to $\bar{p}p \to K^*(890)\bar{K} + cc$, forming a '$K^*$ cross', and an anti-diagonal band due to $\bar{p}p \to \phi(1020)\pi^0$ [cc stands for charge conjugate, here $\bar{K}^*(890)K$]. The combination $K_L K_S$ with C parity = –1 acts like a filter on possible C eigenstates, leaving in this case only a $J^{PC} = 1^{--}$ resonance, the ϕ. Since the whole final state is a C-parity eigenstate, each individual particle K_L, K_S or π^0 being a C-parity eigenstate, there is a phase relation between the two amplitudes $K_L^* K_S$ and $K_S^* K_L$, where $K_{L,S}^*$ means that this K^* decays to $K_{S,L}\pi^0$ (see Appendix). There is no overlap of the three bands, except in the crossing of the vertical and horizontal bands. This is a classic example of a clean Dalitz plot with nothing but three resonances and little interference.

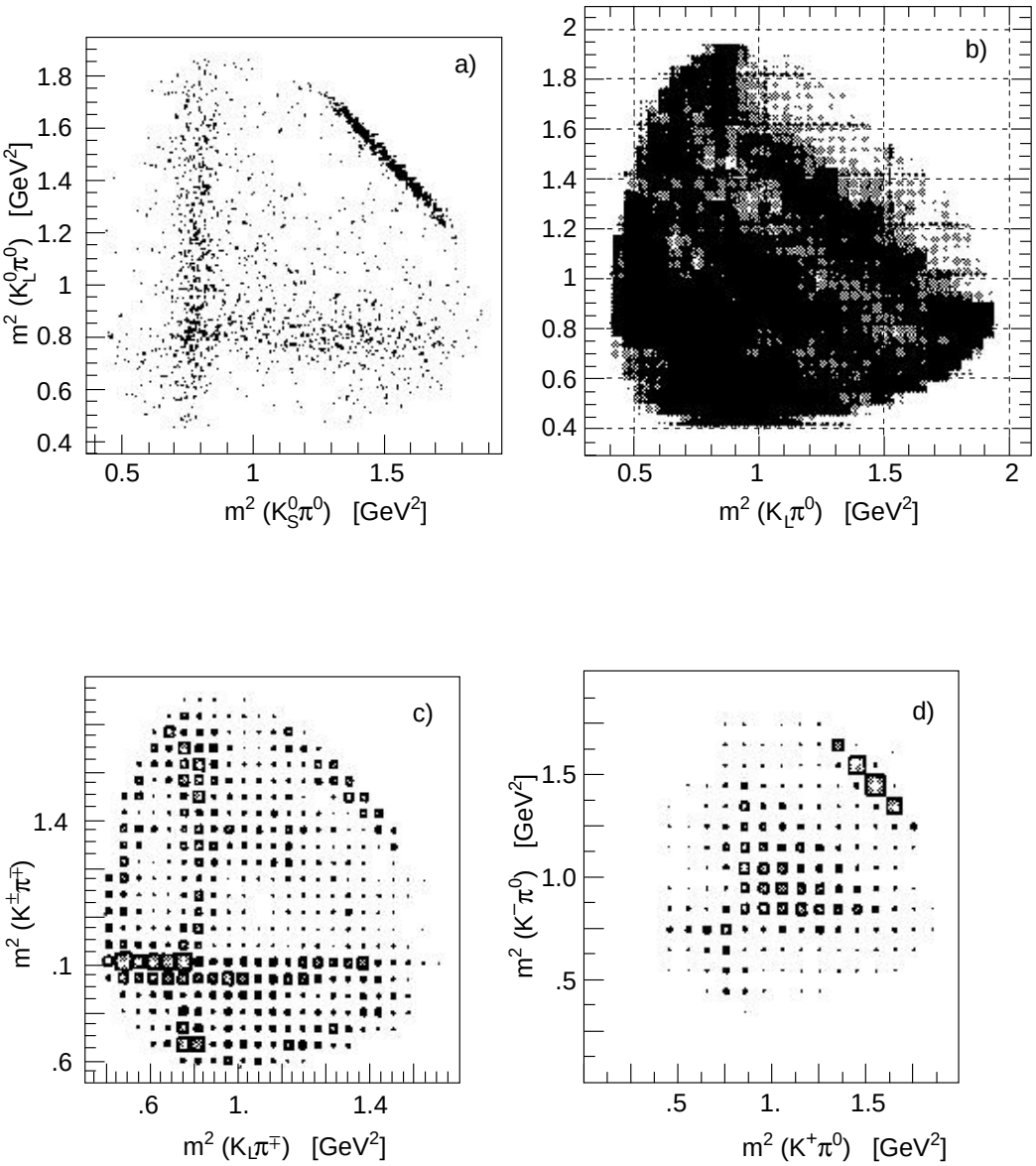

Figure 11: Dalitz plots for four different $\bar{K}K\pi$ final states produced in $\bar{p}p$ annihilation at rest: (a) $\bar{p}p \to K_L K_S \pi^0$; (b) $\bar{p}p \to K_L K_L \pi^0$; (c) $\bar{p}p \to K_L K^{\pm}\pi^{\mp}$; (d) $\bar{p}p \to K^+ K^- \pi^0$. All data are from the Crystal Barrel experiment.

The next example, the Dalitz plot of Fig. 11b for the reaction

$$\bar{p}p \to K_L K_L \pi^0$$

still shows the $K^*(890)$ as the dominant neutral $K\pi$ resonance, but different $\bar{K}K$ resonances are now filtered out: those with positive C parity, i.e. f_0's and a_0's. Here interference plays a much stronger role. Through interference with the diagonal $\bar{K}K$ bands, the upper parts of the K^* cross are almost wiped out.

Now, let us see (Fig. 11c) what happens in the final state with a charged pair of Ks, where ϕ's and f_0's cannot be produced (see Table 4). This Dalitz plot is ideally suited to extract the strength of a_0 and a_2 production, without the problem of overlap with nearby f_0 and f_2. Some indications of diagonal activity which interferes with the K* cross can be seen.

The last Dalitz plot (Fig. 11d) shows a fascinating alternative interference pattern, although the plot is a little crude. Interference between the K* cross and the diagonal a's and f's is constructive in the upper right and lower left quarter and destructive elsewhere. It changes sign on the middle lines of the cross, e.g. the left side of the vertical K^0_S band is eaten up in the upper part and the right side in the lower part.

These Dalitz plots, not completely analysed as yet, show in a qualitative way the power of interference. It was stated above that interference adds another complication. Whilst true, this sounds too negative a statement. Once interferences are understood and the right formalism is found to describe them, they are a powerful tool in determining amplitudes. Interferometry is in general one of the finest and most powerful techniques in physics and elsewhere. It was by measuring interference of X-rays that the double helical structure of the DNA was discovered; by comparing the X-ray picture and the corresponding structure of DNA (Fig. 12) it can be seen that some experience is needed to interpret these patterns.

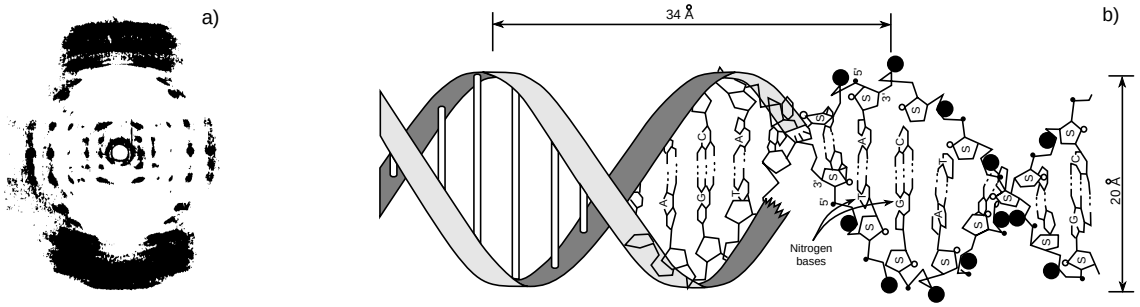

Figure 12: (a) X-ray diffraction photograph of crystalline DNA by Rosalind Franklin and (b) the structure of DNA.

4 BIOGRAPHIES OF STRANGE CHARACTERS

The sector of strange mesons is particularly rich in experimental information, mainly thanks to many productive years of the LASS experiment at SLAC. Among the lowest lying kaons, only the first radially-excited pseudoscalar, $K(1460)$, needs confirmation. An extraordinarily large number of higher kaon excitations has also been found. I will discuss in the following sections only some of the open problems for mesons with hidden strangeness. Let us first discard those mesons in this sector which apparently do not pose any problem. These are the ϕ mesons — ground state and first radial excitation

are confirmed — and the tensor meson $f_2'(1525)$. For the vector ground state, and first excited state, and for the lowest tensor state, the whole nonets are in ideal shape; ideal in a general and a specific sense, in that complete information is available and the two isoscalars are ideally mixed, i.e. almost pure $\bar{s}s$ and $(\bar{u}u + \bar{d}d)$. The nonet mixing angles can be found on p. 1320 of the Review of Particle Properties [3], hereinafter referred to as the 'bible'.

4.1 Who or where is f_0'?

The scalar nonet is a mystery and, in particular, the lack of a confirmed f_0' seems scandalous. Since this nonet is the subject of lectures by T. Burnett (0^+ and 2^+ mesons) and also by M. Boutemeur (Glueballs and Hybrids), I will restrict discussion to the question where or what is the isoscalar scalar meson consisting dominantly of $\bar{s}s$, which should be detected via the preferred decay mode into $\bar{K}K$ (for instance K_SK_S, K_LK_L).

According to the 'bible' there were three confirmed f_0 mesons in 1994: $f_0(980)$, $f_0(1300)$ and $f_0(1590)$. The $f_0(1500)$ [16], not in the 1994 list of confirmed mesons, will certainly make it into the next edition of the 'bible' and $f_0(1370)$ [18] will probably be merged with the $f_0(1300)$. Reading the 'Note on S-wave $\pi\pi$, $\bar{K}K$ and $\eta\eta$ interactions' in the 'bible' [3], p. 1478, one gets an idea of how complicated and interesting the real situation is and how different its interpretation may be from what we think now. The dominant prejudices are that $f_0(980)$ is a $\bar{K}K$ molecule; $f_0(1300)$ is a good, normal meson, mainly $\bar{u}u + \bar{d}d$; $f_0(1500)$ is marketed as a glueball and $f_0(1590)$, which had been one of the best glueball candidates before the arrival of $f_0(1500)$, has been pushed into a corner. In a recent letter by Amsler and Close [19], the $f_0(1590)$ is not even mentioned once.

According to prejudice, the f_0' should be about 200–300 MeV (twice the quark mass difference $m_s - m_u$) heavier than the $f_0(1300)$ and thus be situated around 1500 MeV. There is a candidate for a f_0' which has been seen in only two experiments and therefore omitted from the summary table in the 'bible'. Figure 13 shows the modest evidence presented by the LASS collaboration [20] for a K_SK_S S-wave resonance f_0'. The perfect degeneracy with the strong peak $f_2'(1525)$ seen in the D wave is suspicious, although there is no strong reason to exclude the possibility that f_0' and f_2' are indeed degenerate, see Fig. 3. The possibility that this resonance has the same origin as the $f_0(1500)$ of the Crystal Barrel is not excluded either.

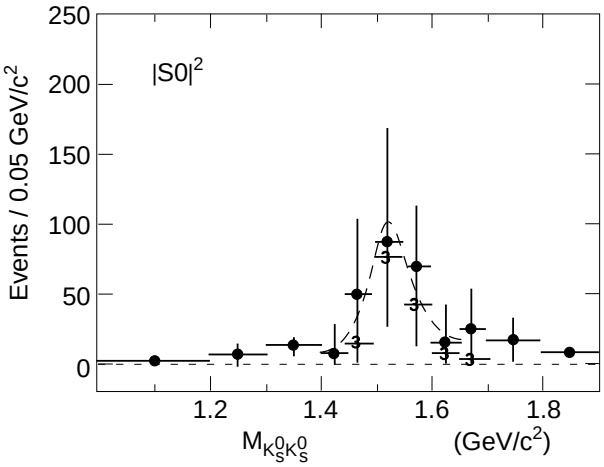

Figure 13: Invariant mass distribution for S-wave K_SK_S produced in $K^-p \to K_SK_S\Lambda$ (LASS experiment).

From a bubble chamber experiment ($\bar{p}d$), an upper limit has been published for the production of a $f_0(1500)$ decaying to $K_S K_S$ [21]. This experiment has by the way, observed the first indication of this resonance, which they called f_2', in $\pi^+\pi^-$ and it has been given a tentative assignment J = 0, which turned out to be correct! Their limit on the $K_S K_S$ decay can be translated into a conservative upper limit of 0.1 for the ratio of phase-space corrected branching ratios $f_0(1500) \to \bar{K}K$ to $f_0(1500) \to \pi\pi$. This value was used in the letter [19] as the key result to prove that the $f_0(1500)$ found by Crystal Barrel is a glueball. We discuss their argument below for the sake of its didactic value.

The evidence for $f_0(1500)$ being a scalar glueball is based on the ratios of decay branching ratios for $f_0(1500)$,

$$\begin{array}{ccccccc} \pi\pi & : & \eta\eta & : & \eta\eta' & : & \bar{K}K \\ 1.00 & : & 0.27 \pm 0.11 & : & 0.19 \pm 0.08 & : & < 0.1(95\%\ CL) \quad , \end{array}$$

corrected for phase space. The first three branching ratios were measured by the Crystal Barrel experiment, the last one is the limit from the bubble chamber experiment [21].

The key point is that the branching ratio into $\bar{K}K$ is too low in comparison with the other numbers to be accommodated by any quark composition (mixing angle) of normal mesons. This can be seen in Fig. 14, which shows the relative invariant couplings (phase-space corrected decay branching ratios predicted from flavour-SU(3) symmetry) as a function of the octet–singlet mixing angle for the decays of a f_0 into various pairs of pseudoscalars. The $\eta\eta/\pi\pi$ ratio puts us in the range $90° \leq \theta \leq 140°$ (the small range near $\theta = 0$ allowed by this ratio is excluded since it demands a dominant $\bar{K}K$ decay). The ratio $\eta\eta/\eta\eta'$, which can be anything between 0.6 and 3, favours the region $110° \leq \theta \leq 135°$. By rough estimation, the mixing angle should therefore be around 120°–130°. But then the $\bar{K}K/\pi\pi$ ratio ought to be between 0.2 and 0.5, clearly larger than the limit of reference [21].

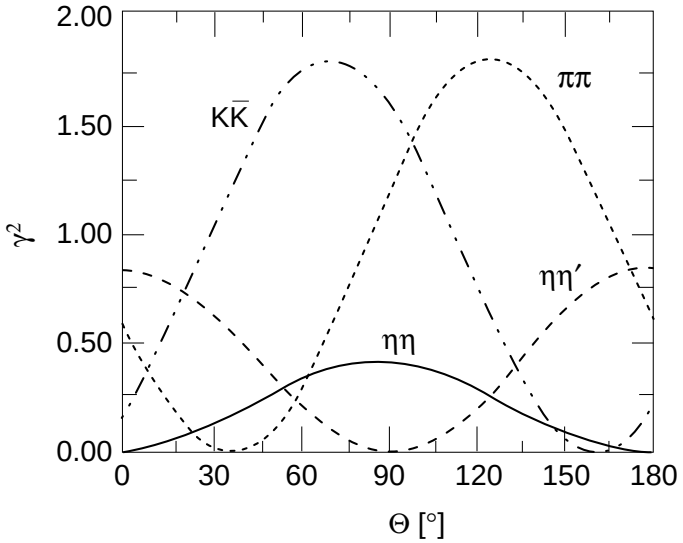

Figure 14: Relative couplings (arbitrary units) to $\pi\pi$, $\eta\eta$, $\eta\eta'$, $\bar{K}K$ as a function of the nonet mixing angle from reference Amsler and Close.

It remains to be seen what the analyses of the Dalitz plots in Fig. 11b–d will teach us about contributions of $f_0(f_0')$. A preliminary analysis of the $K_L K_L \pi^0$ and $K_S K_S \pi^0$

Dalitz plots has found a f_0 resonance at 1600 MeV with mass and width compatible with the GAMS $f_0(1590)$ [22]. Its contribution to the intensity of the final state was 30%, which combined with the branching ratio

$$BR(\bar{p}p \rightarrow K_S K_S \pi^0) = (7.8 \pm 0.6)10^{-4} \quad ,$$

yields a branching ratio

$$BR(\bar{p}p \rightarrow f_0(1600)\pi^0 \rightarrow K_S K_S \pi^0) = (2.3 \pm 0.3)10^{-4} \ .$$

Now let us assume that $f_0(1500)$ and $f_0(1600)$ are the same particles, since rumours have spread that representatives of GAMS and Crystal Barrel at a recent meeting on a remote island agreed that the GAMS $f_0(1590)$ and the Crystal $f_0(1500)$ can be identical. Whilst this assumption may not be completely absurd, it should not be taken too seriously at present. Comparing the last branching ratio with

$$BR(\bar{p}p \rightarrow f_0(1500)\pi^0 \rightarrow 3\pi^0) = (8 \pm 3)10^{-3} \quad ,$$

we obtain a ratio of branching ratios

$$BR(f_0(1600) \rightarrow K_S K_S)/BR(f_0(1500) \rightarrow \pi\pi) \approx 0.3 \quad .$$

After correcting for phase space ($p_K/p_\pi = 580/750$) and applying a weight of 4 to the Ks and of 3 to the π's we get

$$BR(f_0(1500/1600) \rightarrow \bar{K}K)/BR(f_0(1500/1600) \rightarrow \pi\pi) \approx 0.5 \quad .$$

Thus, this object $f_0(1500)/(1600)$ could indeed be a $\bar{q}q$ meson with a mixing angle of 120°.

However, we may have been presumptuous since analysis of all data is not yet complete. Determining the nature of the $f_0(1500)$ and searching for the $\bar{s}s$ partner f_0' of $f_0(1300)$ remains a great challenge.

The main content of this section was based on a common prejudice: the $f_0(980)$, although it prefers to decay into $\bar{K}K$, cannot be the $\bar{s}s$ meson f_0' because its mass is too low relative to that of the $\bar{u}u + \bar{d}d$ resonance $f_0(1300)$. In a recent, highly-sophisticated paper (discussed in detail by Burnett in his lectures) Törnqvist [23] presents a coherent interpretation of the lowest scalar mesons $f_0(980), a_0(980), K_0^*(1430)$ and $f_0(1300)$ within the framework of the unitarized quark model. The $f_0(980)$ emerges as a dominantly $\bar{s}s$ resonance with a large $\bar{K}K$ component. If all this is true, the $f_0(1500/1600)$ has to be considered as candidate for a radial excitation! Or, alternatively, it may be produced by a similar mechanism as $f_0(980)$ since new strong thresholds ($\rho\rho, \omega\omega$) are opened just around this mass.

4.2 The radially-excited pseudoscalar η'

The lower of the excited η mesons, $\eta(1285)$, has been detected in four experiments. It has been seen to decay into $\eta\pi^+\pi^-$ and $a_0\pi$. It is natural to identify this meson with a dominantly $(\bar{u}u + \bar{d}d)$ radial excitation of the $\eta(547)$.

Under the entry $\eta(1440)$ in the 'bible' there is a plethora of experimental references and a special 'Note on the $\eta(1440)$'. This material is too extensive to be covered in a lecture such as this.

In short, an E meson with $J^{PC}(I^G) = 0^{-+}(0^+)$ was first seen in a bubble chamber experiment $\bar{p}p \to (\bar{K}K\pi)\pi\pi$ at a mass of 1425 MeV with a width of 80 MeV by Baillon et al. [24], decaying via $a_0(980)\pi$ and KK^* to $\bar{K}K\pi$. Some time later, confusion was created when in the reaction $\pi^- p \to (\bar{K}K\pi)n$ a 1^{++} resonance was observed [25] at almost exactly the same mass, also decaying to $\bar{K}K\pi$. It was decided that the E meson was a f_1 rather than a η. However, years later a 0^{-+} resonance was rediscovered in radiative J/ψ decays $[J/\psi \to (\bar{K}K)\gamma]$ and was called 'iota' (ι). Two groups (Mark III [26] and DM2 [27]) studying radiative J/ψ decays concluded that there were two overlapping 0^{-+} resonances, one at 1420 MeV decaying into $\bar{K}K\pi$ and $a_0\pi$, and another at 1490 MeV mainly decaying into $\bar{K}K\pi$ (see Fig. 15a and b and Fig. 16b–d).

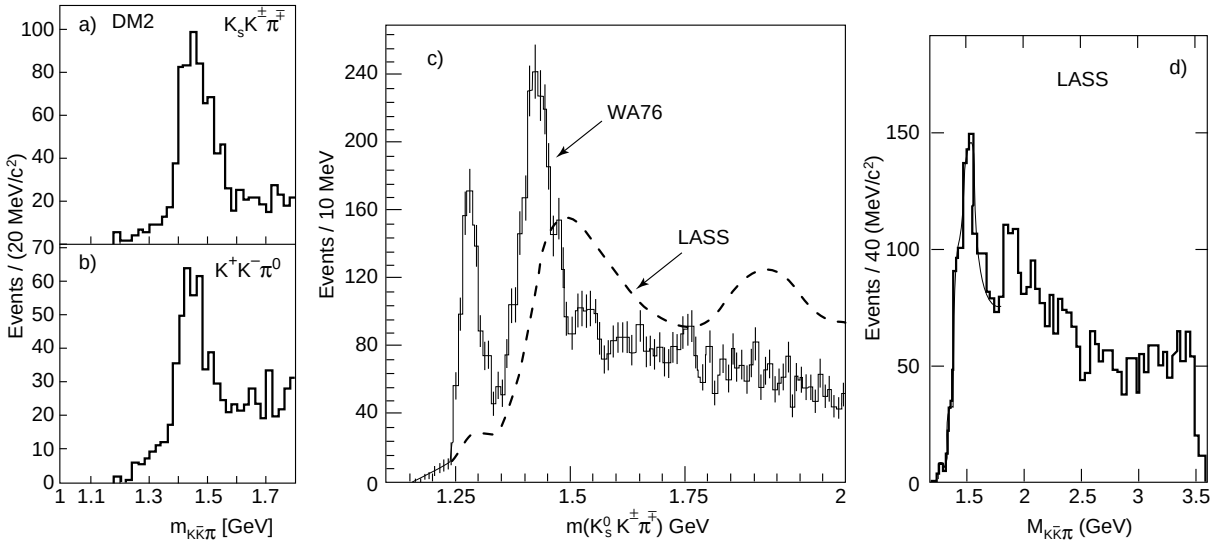

Figure 15: Measured invariant $\bar{K}K\pi$ mass spectra from three experiments: (a) and (b) DM2 (J/ψ radiative decay) [27]; (c) WA76 [28] ($\pi^- p \to K_S K^\pm \pi^\mp n$) compared with LASS [29] (dashed line); and (d) LASS [29] ($K^- p \to K_S K^\pm \pi^\mp \Lambda$).

Today, the most likely interpretation of all the results is that there are indeed, in addition to two f_1 mesons at 1420 and 1510 MeV, two 0^{-+} (η or η') mesons in this narrow mass range, and perhaps an h_1' meson as well, see the following section in Fig. 3e only one η' state has been plotted.

Recently, even more experimental data has been obtained, which has to be inserted into the framework known as the 'E/iota' puzzle. Some of the data come from the Crystal Barrel [30]: a 0^{-+} resonance has been observed in $\bar{p}p \to \eta\pi^0\pi^0\pi^+\pi^-$ at rest, decaying into $\eta\pi\pi$ via $a_0\pi$ and $\eta(\pi\pi)_S$ and having a mass of 1409 $\pm$ 3 MeV and a width of 86 $\pm$ 10 MeV; it is perfectly consistent with the lower iota. Other data come from the OBELIX experiment, which studied $\bar{p}p \to \bar{K}K\pi\pi\pi$ with larger statistics than the earlier bubble chamber experiment [31]. OBELIX finds evidence for two pseudoscalar states, at 1406 and 1499 MeV with widths 75 and 240 MeV, respectively; the first one decays mainly via $a_0\pi$, the second one via K^*K to $\bar{K}K\pi$, in agreement with the results from radiative J/ψ decays.

4.3 The axial-vector meson ground-state h_1'

The experimental data are rather restricted for h_1 and h_1'. A very wide $\rho\pi$ resonance with $J^{PC} = 1^{+-}(I = 0)$ has been seen in three experiments at a mass of 1170 MeV. The

width is $\approx$ 340 MeV! This resonance is identified with the dominantly $(\bar{u}u + \bar{d}d)$ meson h_1. The $\bar{s}s$ partner h_1' is expected to decay dominantly to $\bar{K}K\pi$. So far, in a single experiment, by the LASS collaboration, a candidate has been observed in $K^-p \to K_S K^\pm \pi^\mp \Lambda$ at a mass $\approx$ 1380 MeV, with a width $\approx$ 80 MeV, decaying into $K^*\bar{K}$ $(+cc)$ [29]. The invariant mass distribution of $K_S K^\pm \pi^\mp$ shows a prominent peak around 1.5 GeV (Fig. 15d), and more structure at higher masses, not discussed here. The partial wave analysis finds that the 1.5 GeV mass region is dominated by $K^*\bar{K} + cc$ with $J^P = 1^+$. However, the structure cannot be due to a single resonance. The sign of the interference of the two K^* bands changes between the two $\bar{K}K\pi$ mass windows, 1.34–1.46 GeV and 1.46–1.58 GeV (Fig. 1b and c of [29]). The interference appears to be destructive at the lower mass, indicating a G = –1 object there, whilst for the higher mass it is constructive as expected for G = +1, see Fig. 18e and f. From the measured $K^0\bar{K}^*$ and $\bar{K}^0K^*$ intensities and the interference between these two amplitudes, the intensity of the G-parity eigenstates has been extracted and is shown in Fig. 17a and b; the authors conclude that two 1^+ resonances are observed in this mass region, one with G = –1 and the other with G = +1. Arguing that isospin = 0 is more likely in the peripheral hypercharge exchange reaction $K^-p \to K_S K^\pm \pi^\mp \Lambda$ and hence G = C, and that the production of $\bar{s}s$ dominates in this reaction, it is then claimed that the h_1' ground state (Fig. 17b) and an $f_1(1520)$ meson (Fig. 17a) have been observed.

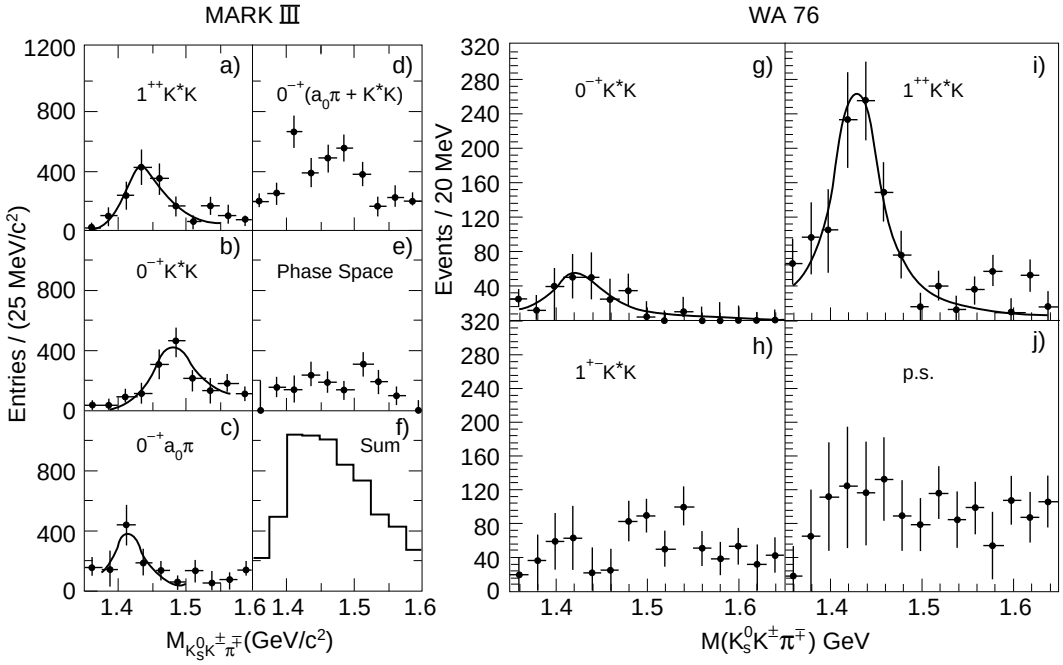

Figure 16: Results of partial wave analyses: (a)–(f) from Mark III $(J/\psi \to \gamma K_S K^\pm \pi^\mp n)$ [26]; and (g)–(j) from WA76 $(\pi^- p \to K_S K^\pm \pi^\mp n)$ [28].

4.4 Axial-vector mesons f_1'

According to the 'bible' there are three narrow f_1 resonances in the mass range 1250–1550 MeV where only two quark model mesons are expected: the $f_1(1285)$, $f_1(1420)$ and $f_1(1510)$, with widths of 24, 52 and 35 MeV, respectively. The first one decays with probabilities of 54% to $\eta\pi\pi$ [mainly $a_0(980)\pi$], 30% to 4π and 10% to $\bar{K}K\pi$. It appears to be a reliable $\bar{u}u + \bar{d}d$ quark meson. The other two mesons have both been observed

exclusively through their decay into $\bar{K}K\pi$; thus they are a priori candidates for $\bar{s}s$ mesons. The $f_1(1510)$ was seen in the LASS experiment, which also observed the h_1' meson [29], and in two other experiments. The $f_1(1420)$ has been identified in many different experiments in $\bar{p}p$ annihilation, J/ψ decays, $\gamma\gamma$ collisions, and in πp interactions (see, for instance, Fig. 15a–c [28], Fig. 16a and i [28] and Fig. 17d [25]).

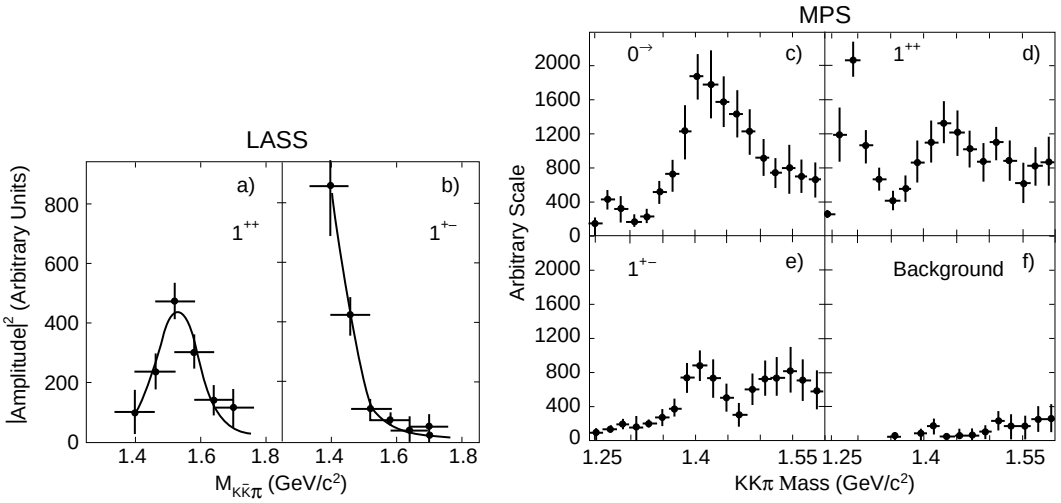

Figure 17: Results from partial wave analyses: (a) and (b) from LASS ($K^-p \to K_S K^\pm \pi^\mp \Lambda$) [29]; (c)–(f) from MPS ($\pi^-p \to K_S K^+ \pi^- n$) [25].

On the one hand, it is completely excluded in the quark model to have two narrow states with identical quantum numbers only 90 MeV apart. Moreover (still on the same hand), the situation reminds us of that for the $\eta(1410)/\eta(1490)$ and makes us wonder what the presence of these doublets might signify. The 'bible' quotes as the preferred interpretation that one of them, the $f_1(1420)$, is not a normal meson, whilst the $f_1(1510)$ is the dominantly $\bar{s}s$ f_1' meson.

On the other hand, a close inspection and comparison on the same mass scale of the LASS [29] and the WA76 [28] data (Fig. 15c) makes one wonder whether these two f_1 mesons are really different from each other. Why is the $f_1(1420)$ meson only seen in one experiment and not in the other and vice versa for the $f_1(1510)$? The questions raised here at the end of the lectures do not really concern the $f_1(1420)/f_1(1510)$ problem. (I am not in a position, at present, to judge the quality and consistency of various experiments). But they do have a rather general didactic purpose. After having referred to the Review of Particle Properties [3] of the Particle Data Group throughout these lectures as a bible for the meson and baryon spectroscopist, it is a moral duty to say at least once that even this bible should sometimes be questioned. It is **our** bible; therefore, whilst we try to get as many of the miracles that we, the experimentalists achieve into this book, we should not believe that every miracle that has been included in the meson (or baryon) summary table, exists beyond doubt.

APPENDIX: C AND G PARITY EIGENSTATES OF $\bar{K}K$ PAIRS

We adopt the following sign convention for the charge conjugation C and the G-parity operation [2]:

$Cu = +\bar{u}$	$Cd = +\bar{d}$	$Cs = +\bar{s}$	$C\bar{u} = +u$	$C\bar{d} = +d$	$C\bar{s} = +s$
$Gu = +\bar{d}$	$Gd = -\bar{u}$	$Gs = +\bar{s}$	$G\bar{d} = -u$	$G\bar{u} = +d$	$G\bar{s} = +s$

where C is the charge conjugation operator and $G = e^{i\pi I_y} C$.
The flavour wave functions of Table 4.2 in [2] are adopted. Thus, for instance:

$$\begin{aligned}
\pi^+ &= +[u(1)\bar{d}(2) + \bar{d}(1)u(2)]/\sqrt{2} \\
\pi^0 &= +[d(1)\bar{d}(2) - u(1)\bar{u}(2) + \bar{d}(1)d(2) - \bar{u}(1)u(2)]/2 \\
K^+ &= +[u(1)\bar{s}(2) + \bar{s}(1)u(2)]/\sqrt{2} \\
K^- &= -[s(1)\bar{u}(2) + \bar{u}(1)s(2)]/\sqrt{2} \\
K^0 &= +[d(1)\bar{s}(2) + \bar{s}(1)d(2)]/\sqrt{2} \\
\bar{K}^0 &= -[s(1)\bar{d}(2) + \bar{d}(1)s(2)]/\sqrt{2} \\
\rho^+ &= +[u(1)\bar{d}(2) - \bar{d}(1)u(2)]/\sqrt{2} \\
K^{+*} &= +[u(1)\bar{s}(2) - \bar{s}(1)u(2)]/\sqrt{2} \\
K^{-*} &= -[s(1)\bar{u}(2) - \bar{u}(1)s(2)]/\sqrt{2} \\
K^{0*} &= +[d(1)\bar{s}(2) - \bar{s}(1)d(2)]/\sqrt{2} \\
\bar{K}^{0*} &= -[s(1)\bar{d}(2) - \bar{d}(1)s(2)]/\sqrt{2} \quad .
\end{aligned}$$

The following signs for the action of C, G and G^2 on pseudoscalar mesons are obtained:

$C\pi^0 = +\pi^0$	$G\pi^0 = -\pi^0$	$G^2\pi^0 = +\pi^0$
$C\pi^+ = -\pi^-$	$G\pi^+ = -\pi^+$	$G^2\pi^+ = +\pi^+$
$C\pi^- = -\pi^+$	$G\pi^- = -\pi^-$	$G^2\pi^- = +\pi^-$
$CK^+ = -K^-$	$GK^+ = -\bar{K}^0$	$G^2K^+ = -K^+$
$CK^- = -K^+$	$GK^- = -K^0$	$G^2K^- = -K^-$
$CK^0 = -\bar{K}^0$	$GK^0 = +K^-$	$G^2K^0 = -K^0$
$C\bar{K}^0 = -K^0$	$G\bar{K}^0 = +K^+$	$G^2\bar{K}^0 = -\bar{K}^0$

For the strange **vector** mesons one obtains just the opposite signs for C and G:

$CK^{+*} = +K^{-*}$	$GK^{+*} = +\bar{K}^{0*}$	$G^2K^{+*} = -K^{+*}$
$CK^{-*} = +K^{+*}$	$GK^{-*} = +K^{0*}$	$G^2K^{-*} = -K^{-*}$
$CK^{0*} = +\bar{K}^{0*}$	$GK^{0*} = -K^{-*}$	$G^2K^{0*} = -K^{0*}$
$C\bar{K}^{0*} = +K^{0*}$	$G\bar{K}^{0*} = -K^{+*}$	$G^2\bar{K}^{0*} = -\bar{K}^{0*}$

The action of G^2 causes a minus sign for all kaons. A 2π rotation in isospace for an isospin $1/2$ particle has the same effect as the corresponding rotation in space on the wave function of a spin $1/2$ particle.

Pairs of $K\bar{K}$.

Here we are mainly interested in the C and isospin eigenstates or, alternatively, G eigenstates. The $|I, I_z = 0, 0\rangle$ and $|I, I_z = 1, 0\rangle$ wave functions of $\bar{K}K$, combinations of an I doublet with an I antidoublet, such as ρ^0 and ω, or π^0 and η, are

$$\begin{aligned}
|I, I_z = 0, 0\rangle &= |K^0(1)\bar{K}^0(2) + K^+(1)K^-(2)\rangle/\sqrt{2} \\
|I, I_z = 1, 0\rangle &= |K^0(1)\bar{K}^0(2) - K^+(1)K^-(2)\rangle/\sqrt{2}.
\end{aligned}$$

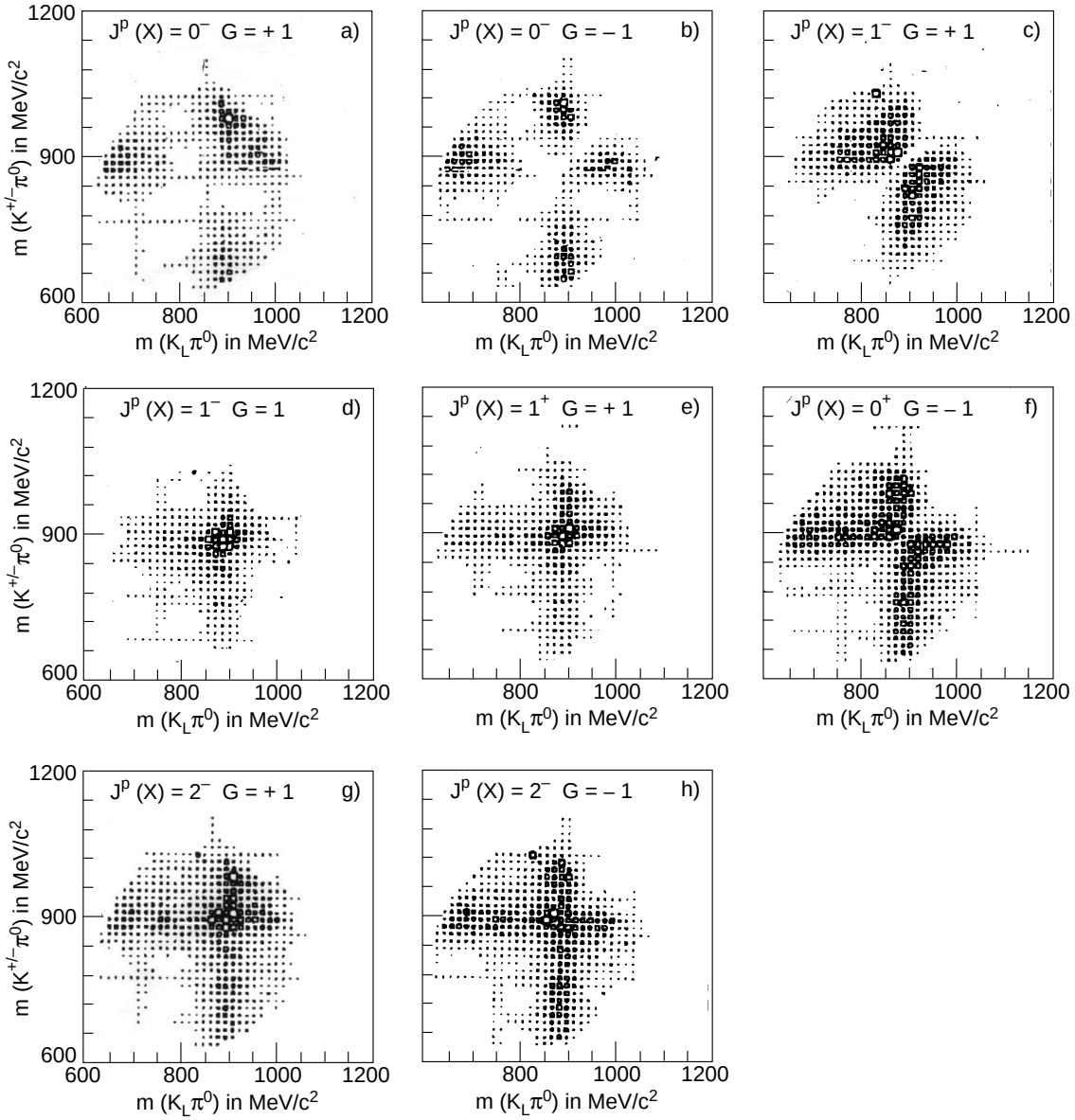

Figure 18: Dalitz plots (Monte Carlo generated by C. Kolo) showing the interference patterns for various J^P and G combinations of a meson with mass 1530 MeV decaying into $\bar{K}K\pi$ via $K^*\bar{K} \pm cc$. J^{PG} = (a) 0^{-+}, (b) 0^{--}, (c) 1^{-+}, (d) 1^{--}, (e) 1^{++}, (f) 1^{+-}, (g) 2^{-+}, (h) 2^{--}.

(Note that the signs are opposite to those of the standard Clebsch–Gordan coefficients (see Section 2.4 for an explanation). These are not yet eigenfunctions of C, but from the action of C on the Ks the eigenstates can be constructed. (In the following, the particle indices in brackets which refer to a given spatial state of one particle will be omitted).

I	I_z	C	$\bar{K}K$ flavour wave functions	G	L
0	0	$+1$	$[K^0\bar{K}^0 + K^+K^- + \bar{K}^0K^0 + K^-K^+]/2$	$+1$	$0, 2, ...$
0	0	-1	$[K^0\bar{K}^0 + K^+K^- - (\bar{K}^0K^0 + K^-K^+)]/2$	-1	$1, 3, ...$
1	0	$+1$	$[K^0\bar{K}^0 - K^+K^- + (\bar{K}^0K^0 - K^-K^+)]/2$	-1	$0, 2, ...$
1	0	-1	$[K^0\bar{K}^0 - K^+K^- - (\bar{K}^0K^0 - K^-K^+)]/2$	$+1$	$1, 3, ...$

What do these eigenfunctions tell us? For meson–antimeson pairs, parity P, C-parity and G-parity are related to L, S and I by similar relations as for fermion–antifermion pairs (we use capital L here for the orbital angular momentum, S for the total spin of the pair):

$$P = (-1)^L$$

$$C = (-1)^{L+S}$$

$$G = (-1)^I C = (-1)^{I+L+S}.$$

Thus it can be seen from the expression for P (or more directly, from the symmetries of the wave function with respect to particle interchange) that the first and third of the 4 eigenfunctions correspond to a wave function with L = 0, 2, ... and that the remaining two have odd L (see the last column). This can be confirmed with the relation for G, or directly by applying the rules listed above for the action of G on the Ks and $\bar{K}$s, that G takes the values given in the next to last column.

Similarly, the wave functions for other pairs, like KK^*, K^*K^* can be obtained. The C, I and G eigenstates for neutral ($I_z = 0$) pairs of $K^*\bar{K}^* + cc$ have the same sequence of signs:

I	I_z	C	$K^*\bar{K}^*$ flavour wave functions	G	$S + L$
0	0	$+1$	$[K^{0*}\bar{K}^{0*} + K^{+*}K^{-*} + \bar{K}^{0*}K^{0*} + K^{-*}K^{+*}]/2$	$+1$	$0, 2, ...$
0	0	-1	$[K^{0*}\bar{K}^{0*} + K^{+*}K^{-*} - (\bar{K}^{0*}K^{0*} + K^{-*}K^{+*})]/2$	-1	$1, 3, ...$
1	0	$+1$	$[K^{0*}\bar{K}^{0*} - K^{+*}K^{-*} + (\bar{K}^{0*}K^{0*} - K^{-*}K^{+*})]/2$	-1	$0, 2, ...$
1	0	-1	$[K^{0*}\bar{K}^{0*} - K^{+*}K^{-*} - (\bar{K}^{0*}K^{0*} - K^{-*}K^{+*})]/2$	$+1$	$1, 3, ...$

For pairs of $K\bar{K}^*, K^*\bar{K}$, the signs in the middle are reversed because the C parity of K^* is opposite to that of K:

I	I_z	C	$K\bar{K}^*(\bar{K}^0K^*)$ flavour wave functions	G
0	0	$+1$	$[K^0\bar{K}^{0*} + K^+K^{-*} - (\bar{K}^0K^{0*} + K^-K^{+*})]/2$	$+1$
0	0	-1	$[K^0\bar{K}^{0*} + K^+K^{-*} + (\bar{K}^0K^{0*} + K^-K^{+*})]/2$	-1
1	0	$+1$	$[K^0\bar{K}^{0*} - K^+K^{-*} - (\bar{K}^0K^{0*} - K^-K^{+*})]/2$	-1
1	0	-1	$[K^0\bar{K}^{0*} - K^+K^{-*} + (\bar{K}^0K^{0*} - K^-K^{+*})]/2$	$+1$

In the last case, the four terms in the sum seem to be physically distinguished, not just permutations of particle indices as in the case of $K\bar{K}$ and $K^*\bar{K}^*$. However, the final states resulting from the decay of the K^*s overlap in some regions of phase space and therefore interference between the various terms takes place. We need additional relations to obtain

the correct signs of interference in the final state, namely those which connect the various K^*s with their decay products:

$$\begin{aligned} K^{+*} &= -\sqrt{1/3}(K^+\pi^0) + \sqrt{2/3}(K^0\pi^+) \\ K^{-*} &= +\sqrt{1/3}(K^-\pi^0) + \sqrt{2/3}(\bar{K}^0\pi^-) \\ K^{0*} &= +\sqrt{1/3}(K^0\pi^0) - \sqrt{2/3}(K^+\pi^-) \\ \bar{K}^{0*} &= -\sqrt{1/3}(\bar{K}^0\pi^0) - \sqrt{2/3}(K^-\pi^+). \end{aligned}$$

Here, we have used standard Clebsch–Gordan coefficients for the isospin coupling **with two exceptions** where the signs are opposite [32]: the K^- and K^{-*}, which contain the $\bar{u}$ quark, have to be given a minus sign, consistent with the change in sign of the isospin wave functions of $\bar{K}K$ pairs (see above). In the old literature, see for instance [33, 34], standard Clebsch–Gordan coefficients were used throughout, which may lead to some confusion today. However, their final result for the sign of interference in the final state is consistent with ours.

Since the experiments identify and distinguish certain charge combinations in the final state, for instance, in the case of KK^*, the combination $K^+K^0\pi^-$ (with $I = 1$ or $0, I_z = 0$) or $K^0K^-\pi^0$ (with $I = 1, I_z = -1$), only some of the terms have to be considered at the end. With the formulae given above one can derive the expression for the G-parity eigenstates, valid for arbitrary isospin I and I_z:

$$(\bar{K}K\pi)_G = [K(1)\bar{K}(2)\pi(3) + G\bar{K}(1)K(2)\pi(3)]/\sqrt{1/6} \quad ,$$

where G refers to the state $\bar{K}K\pi$. For specific charge states one obtains, for instance,

$$(\bar{K}K\pi, I = 0 \text{ or } 1, I_z = 0)_G = (K^+\bar{K}^0\pi^- + G\bar{K}^0K^+\pi^-)/\sqrt{1/6}$$

or

$$(\bar{K}K\pi, I = 1, I_z = -1)_G = (K^0K^-\pi^0 + GK^-K^0\pi^0)/\sqrt{1/6} \quad .$$

A positive G parity does not necessarily imply that the interference in the region of overlap is constructive. It depends, in addition, on the spatial, or more specifically on the angular wave function, i.e. its symmetry for interchange of the particle indices. Figure 18 shows some interesting cases of J^{PC}, G eigenstates decaying into KK^*. These patterns can be used to deduce the G parity from the observed interference pattern if J^{PC} is known or assumed to be known.

If the final state under consideration is not a C eigenstate, the G eigenstates are still useful since G is conserved in the strong interaction. We consider as an example pairs with negative charge only, having isospin $I, I_z = 1, -1$, i.e. $K^0K^-, K^{0*}K^{-*}$ and $K^0K^{-*}, K^{0*}K^-$. The G eigenstates can be constructed as above.

$\bar{K}K$ flavour wave functions	G	L
$(K^0K^- + K^-K^0)/\sqrt{2}$	-1	$0, 2, ...$
$(K^0K^- - K^-K^0)/\sqrt{2}$	$+1$	$1, 3, ...$

$K^*\bar{K}^*$ flavour wave functions	G	$S + L$
$(K^{0*}K^{-*} + K^{-*}K^{0*})/\sqrt{2}$	-1	$0, 2, ...$
$(K^{0*}K^{-*} - K^{-*}K^{0*})/\sqrt{2}$	$+1$	$1, 3, ...$

$K K^*$ flavour wave functions	G
$(K^0 K^{-*} + K^- K^{0*})/\sqrt{2}$	$+1$
$(K^0 K^{-*} - K^- K^{0*})/\sqrt{2}$	-1

Now there is another set of expressions which is useful when dealing with neutral Ks. The eigenstates above were expressed in terms of $K^0, \bar{K}^0$, which are eigenstates of the strong interaction but not the mesons seen by the detector. The observed particles are the K_L and K_S, which are to a good approximation C eigenstates, as explained in the text, and to a better approximation CP eigenstates. For our purpose we can use

	C	P	CP
$K_S \approx K_1 = (K^0 + \bar{K}^0)/\sqrt{2}$	-1	-1	$+1$
$K_L \approx K_2 = (K^0 - \bar{K}^0)/\sqrt{2}$	$+1$	-1	-1

The K_1 has exotic quantum numbers $J^{PC} = 0^{--}$! but no defined isospin. For pairs of neutral Ks one finds the following identities by substitution:

$C = +1$	$K^0\bar{K}^0 + \bar{K}^0 K^0$	$K_S K_S - K_L K_L$
$C = -1$	$K^0\bar{K}^0 - \bar{K}^0 K^0$	$K_L K_S - K_S K_L$

It seems as if we have too many terms here since each pair (e.g. $K_S K_S$) is in itself already an eigenstate of C, each particle being a C eigenstate. However, substituting the inverse relations

$$K^0 = (K_S + K_L)\sqrt{2}$$
$$\bar{K}^0 = (K_S - K_L)\sqrt{2}$$

it can be seen that both terms are necessary to cancel pairs with double strangeness, like $K^0 K^0$.

As an example, consider the final state $K_L K_S \pi^0$ for a neutral $K\bar{K}^*$ pair decaying to neutral Ks. The C eigenstates are

$C = +1$	$K^0\bar{K}^{0*} - \bar{K}^0 K^{0*}$	$K_L {K_L}^* - K_S {K_S}^*$
$C = -1$	$K^0\bar{K}^{0*} + \bar{K}^0 K^{0*}$	$K_S {K_L}^* - K_L {K_S}^*$

where $K^*_{L,S}$ is shorthand for $K^0(\bar{K}^0)$ decaying to $K_{L,S}\pi^0$ with angular momentum L = 1. Similarly, for $K^*\bar{K}^*$,

$C = +1$	$K^{0*}\bar{K}^{0*} + \bar{K}^{0*} K^{0*}$	${K_L}^* {K_L}^* - {K_S}^* {K_S}^*$
$C = -1$	$K^{0*}\bar{K}^{0*} - \bar{K}^{0*} K^{0*}$	${K_L}^* {K_S}^* - {K_S}^* {K_L}^*$

Again, each term in the right-hand column is a C eigenstate and the differences are necessary in order to cancel double strangeness terms.

ACKNOWLEDGEMENTS

I wish to thank my co-students and co-teachers, and above all the organizer, David Bugg, for a very stimulating and enjoyable summer school.

References

[1] A. Pais, Niels Bohr's times (Clarendon Press, Oxford, 1991).
[2] F.E. Close, An Introduction to quarks and leptons (Academic Press, London, 1979).
[3] L. Montanet et al., Review of particle properties, Particle Data Group, Phys. Rev. **D50** (1994) 1173.
[4] S. Okubo, Phys. Lett. **5** (1963) 165;
G. Zweig, Report CERN-TH412 (1964);
I. Iizuka, Prog. Theor. Phys. Suppl. **37** (1966) 21.
[5] C. Amsler et al., Phys. Lett. B**333** (1994) 277.
[6] E. Aker et al., Nucl. Instrum. Methods **A321** (1992) 69.
[7] C. Zemach, Phys. Rev. **B133** (1964) 1201; ibid. **B140** (1965) 97, 109.
[8] M. Jacob and G.C. Wick, Ann. Phys. (USA) **7** (1959) 404.
[9] W. Rarita and J. Schwinger, Phys. Rev. **60** (1941) 61.
[10] V. Filippini, A. Fontana, and A. Rotondi, Phys. Rev. **D51** (1995) 2247.
[11] S.U. Chung, Preprint BNL–QGS94–22, submitted to Phys. Rev. D.
[12] J.M. Blatt and V. Weisskopf, Theoretical nuclear physics (Wiley, New York, 1952).
[13] J.D. Jackson, Nuovo Cimento **34** (1964) 1644.
[14] R.N. Cahn and P.V. Landshoff, Nucl. Phys. **B266** (1986) 451.
[15] I.J.R. Aitchison, Nucl. Phys. **A189** (1972) 417.
[16] C. Amsler et al., Phys. Lett. **B355** (1995) 425.
[17] V.V. Anisovich et al., Phys. Rev. **D50** (1994) 1972;
D.V. Bugg et al., Phys. Rev. **D50** (1994) 4412.
[18] C. Amsler et al., Phys. Lett. **B322** (1994) 431.
[19] C. Amsler, F.E. Close, Phys. Lett. **B353** (1995) 385.
[20] D. Aston et al., Nucl. Phys. **B301** (1988) 525.
[21] L. Gray et al., Phys. Rev. **D27** (1983) 307.
[22] H.P. Dietz, PhD thesis, University of Munich 1994.
[23] N.A. Törnqvist, Z. Phys. **C68** (1995) 647.
[24] P. Baillon et al., Nuovo Cimento **50A** (1967) 393.
[25] A. Birman et al. (MPS), Phys. Rev. Lett. **61** (1988) 1557.
[26] Z. Bai et al. (MARKIII), Phys. Rev. Lett. 65 (1990) 2507.
[27] J.-E. Augustin et al. (DM2), Phys. Rev. **D46** (1992) 1951.
[28] T.A. Armstrong et al. (WA76), Z. Phys. **C56** (1992) 29.
[29] D. Aston et al., Phys. Lett. **B201** (1988) 573.
[30] C. Amsler et al. (Crystal Barrel Collaboration), Phys. Lett. **B358** (1995) 389.
[31] A. Bertin et al. (OBELIX Collaboration), Phys. Lett. **B361** (1995) 187.
[32] I thank C. Zupancic for helping me at this point after a long battle with signs.
[33] N. Barash et al., Phys. Rev. **B139** (1965) 1659.
[34] R. Armenteros and B. French, *in* High energy physics, ed. E.H.S. Burhop (Academic Press, New York, London, 1969).